90. J. F. Storz, J. C. Opazo, F. G. Hoffmann, *Mol. Phylogenet. Evol.* **66**, 469–478 (2013).
91. F. G. Hoffmann, J. F. Storz, T. A. Gorr, J. C. Opazo, *Mol. Biol. Evol.* **27**, 1126–1138 (2010).

[1]China National GeneBank, BGI-Shenzhen, Shenzhen 518083, China. [2]Centre for GeoGenetics, Natural History Museum of Denmark, University of Copenhagen, Øster Voldgade 5-7, 1350 Copenhagen, Denmark. [3]CIMAR/CIIMAR, Centro Interdisciplinar de Investigação Marinha e Ambiental, Universidade do Porto, Rua dos Bragas, 177, 4050-123 Porto, Portugal. [4]Department of Behavioral Neuroscience Oregon Health & Science University Portland, OR 97239, USA. [5]Departamento de Biologia, Faculdade de Ciências, Universidade do Porto, Rua do Campo Alegre, 4169-007 Porto, Portugal. [6]Department of Biology, University of Puerto Rico, Av Ponce de Leon, Rio Piedras Campus, JGD 224, San Juan, PR 009431-3360, USA. [7]Trace and Environmental DNA laboratory, Department of Environment and Agriculture, Curtin University, Perth, Western Australia 6102, Australia. [8]Environmental Futures Research Institute, Griffith University, Nathan, Queensland 4121, Australia. [9]Museum of Natural Science, Louisiana State University, Baton Rouge, LA 70803, USA. [10]Marie Bashir Institute for Infectious Diseases and Biosecurity, Charles Perkins Centre, School of Biological Sciences and Sydney Medical School, The University of Sydney, Sydney NSW 2006, Australia. [11]School of Biological Sciences, University of Canterbury, Christchurch 8140, New Zealand. [12]Bioinformatics Group, Department of Computer Science, and Interdisciplinary Center for Bioinformatics, University of Leipzig, Hrtelstrasse 16-18, D-04107 Leipzig, Germany. [13]European Molecular Biology Laboratory, European Bioinformatics Institute, Hinxton, Cambridge CB10 1SD, UK. [14]School of Plant Sciences, BIO5 Institute, University of Arizona, Tucson, AZ 85721, USA. [15]Division of Genetics and Genomics, The Roslin Institute and Royal (Dick) School of Veterinary Studies, The Roslin Institute Building, University of Edinburgh, Easter Bush Campus, Midlothian EH25 9RG, UK. [16]Department of Veterinary Science and Microbiology, University of Arizona, 1117 E Lowell Street, Post Office Box 210090-0090, Tucson, AZ 85721, USA. [17]Laboratoire de Génétique Cellulaire, INRA Chemin de Borde-Rouge, Auzeville, BP 52627 , 31326 CASTANET-TOLOSAN CEDEX, France. [18]Department of Biological Sciences, Science and Engineering 601, University of Arkansas, Fayetteville, AR 72701, USA. [19]Department of Animal Sciences, Oregon State University, Corvallis, OR 97331, USA.

RESEARCH ARTICLE

Whole-genome analyses resolve early branches in the tree of life of modern birds

Erich D. Jarvis,[1]*† Siavash Mirarab,[2]* Andre J. Aberer,[3] Bo Li,[4,5,6] Peter Houde,[7] Cai Li,[4,6] Simon Y. W. Ho,[8] Brant C. Faircloth,[9,10] Benoit Nabholz,[11] Jason T. Howard,[1] Alexander Suh,[12] Claudia C. Weber,[12] Rute R. da Fonseca,[6] Jianwen Li,[4] Fang Zhang,[4] Hui Li,[4] Long Zhou,[4] Nitish Narula,[7,13] Liang Liu,[14] Ganesh Ganapathy,[1] Bastien Boussau,[15] Md. Shamsuzzoha Bayzid,[2] Volodymyr Zavidovych,[1] Sankar Subramanian,[16] Toni Gabaldón,[17,18,19] Salvador Capella-Gutiérrez,[17,18] Jaime Huerta-Cepas,[17,18] Bhanu Rekepalli,[20] Kasper Munch,[21] Mikkel Schierup,[21] Bent Lindow,[6] Wesley C. Warren,[22] David Ray,[23,24,25] Richard E. Green,[26] Michael W. Bruford,[27] Xiangjiang Zhan,[27,28] Andrew Dixon,[29] Shengbin Li,[30] Ning Li,[31] Yinhua Huang,[31] Elizabeth P. Derryberry,[32,33] Mads Frost Bertelsen,[34] Frederick H. Sheldon,[33] Robb T. Brumfield,[33] Claudio V. Mello,[35,36] Peter V. Lovell,[35] Morgan Wirthlin,[35] Maria Paula Cruz Schneider,[36,37] Francisco Prosdocimi,[36,38] José Alfredo Samaniego,[6] Amhed Missael Vargas Velazquez,[6] Alonzo Alfaro-Núñez,[6] Paula F. Campos,[6] Bent Petersen,[39] Thomas Sicheritz-Ponten,[39] An Pas,[40] Tom Bailey,[41] Paul Scofield,[42] Michael Bunce,[43] David M. Lambert,[16] Qi Zhou,[44] Polina Perelman,[45,46] Amy C. Driskell,[47] Beth Shapiro,[26] Zijun Xiong,[4] Yongli Zeng,[4] Shiping Liu,[4] Zhenyu Li,[4] Binghang Liu,[4] Kui Wu,[4] Jin Xiao,[4] Xiong Yinqi,[4] Qiuemei Zheng,[4] Yong Zhang,[4] Huanming Yang,[48] Jian Wang,[48] Linnea Smeds,[12] Frank E. Rheindt,[49] Michael Braun,[50] Jon Fjeldsa,[51] Ludovic Orlando,[6] F. Keith Barker,[52] Knud Andreas Jønsson,[51,53,54] Warren Johnson,[55] Klaus-Peter Koepfli,[56] Stephen O'Brien,[57,58] David Haussler,[59] Oliver A. Ryder,[60] Carsten Rahbek,[51,54] Eske Willerslev,[6] Gary R. Graves,[51,61] Travis C. Glenn,[62] John McCormack,[63] Dave Burt,[64] Hans Ellegren,[12] Per Alström,[65,66] Scott V. Edwards,[67] Alexandros Stamatakis,[3,68] David P. Mindell,[69] Joel Cracraft,[70] Edward L. Braun,[71] Tandy Warnow,[2,72]† Wang Jun,[48,73,74,75,76]† M. Thomas P. Gilbert,[6,43]† Guojie Zhang[4,77]†

To better determine the history of modern birds, we performed a genome-scale phylogenetic analysis of 48 species representing all orders of Neoaves using phylogenomic methods created to handle genome-scale data. We recovered a highly resolved tree that confirms previously controversial sister or close relationships. We identified the first divergence in Neoaves, two groups we named Passerea and Columbea, representing independent lineages of diverse and convergently evolved land and water bird species. Among Passerea, we infer the common ancestor of core landbirds to have been an apex predator and confirm independent gains of vocal learning. Among Columbea, we identify pigeons and flamingoes as belonging to sister clades. Even with whole genomes, some of the earliest branches in Neoaves proved challenging to resolve, which was best explained by massive protein-coding sequence convergence and high levels of incomplete lineage sorting that occurred during a rapid radiation after the Cretaceous-Paleogene mass extinction event about 66 million years ago.

The diversification of species is not always gradual but can occur in rapid radiations, especially after major environmental changes (*1*, *2*). Paleobiological (*3*–*7*) and molecular (*8*) evidence suggests that such "big bang" radiations occurred for neoavian birds (e.g., songbirds, parrots, pigeons, and others) and placental mammals, representing 95% of extant avian and mammalian species, after the Cretaceous to Paleogene (K-Pg) mass extinction event about 66 million years ago (Ma). However, other nuclear (*9*–*12*) and mitochondrial (*13*, *14*) DNA studies propose an earlier, more gradual diversification, beginning within the Cretaceous 80 to 125 Ma. This debate is confounded by findings that different data sets (*15*–*19*) and analytical methods (*20*, *21*) often yield contrasting species trees. Resolving such timing and phylogenetic relationships is important for comparative genomics, which can inform about human traits and diseases (*22*).

Recent avian studies based on fragments of 5 [~5000 base pairs (bp) (*8*)] and 19 [31,000 bp (*17*)] genes recovered new relationships inferred from morphological data (*15*, *23*) and DNA-DNA hybridization (*24*), postulated new relationships, and contradicted many others. Consistent with most previous molecular and contemporary morphological studies (*15*), they divided modern birds (Neornithes) into Palaeognathae (tinamous and flightless ratites), Galloanseres [Galliformes (landfowl) and Anseriformes (waterfowl)], and Neoaves (all other extant birds). Within Neoaves,

they proposed several large new clades, including a waterbird clade containing taxa such as penguins, pelicans, and loons, as well as a landbird clade containing woodpeckers, birds of prey, parrots, and songbirds. Despite these efforts, the relationships among the deepest branches within Neoaves; the positions of a number of chronically challenging taxa such as shorebirds, mousebirds, owls, and the enigmatic hoatzin; and the identification of the first divergence of Neoaves [proposed to have given rise to two equally large clades designated Metaves and Coronaves (25)] remain unresolved.

Although some of the findings of the initial multi-gene studies (8, 17) have since been corroborated with larger sequence (26–28) or transposable element (TE) insertion data sets (29), other proposed clades were not supported (27, 28). Furthermore, complete mitochondrial genome analyses recover different relationships (14, 18) and fail to support higher landbird monophyly [but see (30)]. Some of the differences among studies could arise from gene tree incongruence, possibly due to incomplete lineage sorting (ILS) of those genes (29, 31), nucleotide base composition biases (19), differences between data types (32, 33), or insufficient data (34, 35). Thus, it has been difficult to establish confidence in whether specific avian traits—such as vocal learning, predatory behavior, or adaptations to aquatic or terrestrial habitats—reflect single or multiple independent origins and under what ecological conditions these events have occurred.

A common assumption is that whole-genome data will improve phylogenetic reconstructions, due to the complete evolutionary record within each species' genome and increased statistical power (34, 35). We test this hypothesis through phylogenetic analysis on 48 avian genomes we collected or assembled, representing all commonly accepted extant neognath orders (36, 37) and two palaeognaths, with several nonavian reptiles and human as outgroups.

Species choice, computational developments, and total evidence nucleotide data set

We chose species representing all neoavian orders according to different classifications [see supplementary materials section 1 (SM1)]. These include groups that have been challenging to place within the avian tree, such as the hoatzin, cuckoo-roller, nightjars, mousebirds, mesites, and seriemas (table S1). We also included species postulated to descend from deep nodes in their orders to break up potentially long branches, such as the kea for parrots (Psittaciformes) and the rifleman for songbirds (Passeriformes). We included vocal-learning species (oscine songbirds, hummingbirds, and parrots), used as models for spoken language in humans (38), and their proposed closest vocal-nonlearning relatives (suboscines, swifts, falcons, and/or cuckoos, depending on the tree) to help resolve differences in trees that lead to different conclusions on their independent gains (15, 17, 18, 26, 29, 38, 39). The resulting data set consisted of 45 avian genomes sequenced in part for this project [48 when including previously published species (40–42)] and three nonavian reptiles [American alligator, green sea turtle, and green anole lizard (43)] (table S1), with details reported in (44–52).

We were confronted with computational challenges not previously encountered in smaller-scale phylogenomic studies. Differently annotated genomes complicated the identification of orthologs, and the size of the data matrix made it impossible to use many standard phylogenetic tools. To address these challenges, we generated a uniform reannotation of the protein-coding genes for all avian genomes based on synteny in chicken and zebra finch (SM2). We found that the SATé iterative alignment program (53, 54) yielded more reliable alignments than other algorithms for large-scale data, and we developed alignment-filtering algorithms to remove unaligned and incorrectly overaligned sequences (SM3). We developed ExaML, a computationally more efficient version of the maximum likelihood program RAxML,

[1]Department of Neurobiology, Howard Hughes Medical Institute (HHMI), and Duke University Medical Center, Durham, NC 27710, USA. [2]Department of Computer Science, The University of Texas at Austin, Austin, TX 78712, USA. [3]Scientific Computing Group, Heidelberg Institute for Theoretical Studies, Heidelberg, Germany. [4]China National GeneBank, BGI-Shenzhen, Shenzhen 518083, China. [5]College of Medicine and Forensics, Xi'an Jiaotong University Xi'an 710061, China. [6]Centre for GeoGenetics, Natural History Museum of Denmark, University of Copenhagen, Øster Voldgade 5-7, 1350 Copenhagen, Denmark. [7]Department of Biology, New Mexico State University, Las Cruces, NM 88003, USA. [8]School of Biological Sciences, University of Sydney, Sydney, New South Wales 2006, Australia. [9]Department of Ecology and Evolutionary Biology, University of California, Los Angeles, CA 90095, USA. [10]Department of Biological Sciences, Louisiana State University, Baton Rouge, LA 70803, USA. [11]CNRS UMR 5554, Institut des Sciences de l'Evolution de Montpellier, Université Montpellier II Montpellier, France. [12]Department of Evolutionary Biology, Evolutionary Biology Centre, Uppsala University, SE-752 36 Uppsala Sweden. [13]Biodiversity and Biocomplexity Unit, Okinawa Institute of Science and Technology Onna-son, Okinawa 904-0495, Japan. [14]Department of Statistics and Institute of Bioinformatics, University of Georgia, Athens, GA 30602, USA. [15]Laboratoire de Biométrie et Biologie Evolutive, Centre National de la Recherche Scientifique, Université de Lyon, F-69622 Villeurbanne, France. [16]Environmental Futures Research Institute, Griffith University, Nathan, Queensland 4111, Australia. [17]Bioinformatics and Genomics Programme, Centre for Genomic Regulation, Dr. Aiguader 88, 08003 Barcelona, Spain. [18]Universitat Pompeu Fabra, Barcelona, Spain. [19]Institució Catalana de Recerca i Estudis Avançats, Barcelona, Spain. [20]Joint Institute for Computational Sciences, The University of Tennessee, Oak Ridge National Laboratory, Oak Ridge, TN 37831, USA. [21]Bioinformatics Research Centre, Aarhus University, DK-8000 Aarhus C, Denmark. [22]The Genome Institute, Washington University School of Medicine, St Louis, MI 63108, USA. [23]Department of Biochemistry, Molecular Biology, Entomology and Plant Pathology, Mississippi State University, Mississippi State, MS 39762, USA. [24]Institute for Genomics, Biocomputing and Biotechnology, Mississippi State University, Mississippi State, MS 39762, USA. [25]Department of Biological Sciences, Texas Tech University, Lubbock, TX 79409, USA. [26]Department of Ecology and Evolutionary Biology, University of California Santa Cruz (UCSC), Santa Cruz, CA 95064, USA. [27]Organisms and Environment Division, Cardiff School of Biosciences, Cardiff University Cardiff CF10 3AX, Wales, UK. [28]Key Laboratory of Animal Ecology and Conservation Biology, Institute of Zoology, Chinese Academy of Sciences, Beijing 100101, China. [29]International Wildlife Consultants, Carmarthen SA33 5YL, Wales, UK. [30]College of Medicine and Forensics, Xi'an Jiaotong University Xi'an, 710061, China. [31]State Key Laboratory for Agrobiotechnology, China Agricultural University, Beijing 100094, China. [32]Department of Ecology and Evolutionary Biology, Tulane University, New Orleans, LA 70118, USA. [33]Museum of Natural Science and Department of Biological Sciences, Louisiana State University, Baton Rouge, LA 70803, USA. [34]Center for Zoo and Wild Animal Health, Copenhagen Zoo Roskildevej 38, DK-2000 Frederiksberg, Denmark. [35]Department of Behavioral Neuroscience, Oregon Health and Science University, Portland, OR 97239, USA. [36]Brazilian Avian Genome Consortium (CNPq/FAPESPA-SISBIO Aves), Federal University of Para, Belem, Para, Brazil. [37]Institute of Biological Sciences, Federal University of Para, Belem, Para, Brazil. [38]Institute of Medical Biochemistry Leopoldo de Meis, Federal University of Rio de Janeiro, Rio de Janeiro RJ 21941-902, Brazil. [39]Centre for Biological Sequence Analysis, Department of Systems Biology, Technical University of Denmark Kemitorvet 208, 2800 Kgs Lyngby, Denmark. [40]Breeding Centre for Endangered Arabian Wildlife, Sharjah, United Arab Emirates. [41]Dubai Falcon Hospital, Dubai, United Arab Emirates. [42]Canterbury Museum Rolleston Avenue, Christchurch 8050, New Zealand. [43]Trace and Environmental DNA Laboratory Department of Environment and Agriculture, Curtin University, Perth, Western Australia 6102, Australia. [44]Department of Integrative Biology, University of California, Berkeley, CA 94720, USA. [45]Laboratory of Genomic Diversity, National Cancer Institute Frederick, MD 21702, USA. [46]Institute of Molecular and Cellular Biology, SB RAS and Novosibirsk State University, Novosibirsk, Russia. [47]Smithsonian Institution National Museum of Natural History, Washington, DC 20013, USA. [48]BGI-Shenzhen, Shenzhen 518083, China. [49]Department of Biological Sciences, National University of Singapore, Republic of Singapore. [50]Department of Vertebrate Zoology, National Museum of Natural History, Smithsonian Suitland, MD 20746, USA. [51]Center for Macroecology, Evolution and Climate, Natural History Museum of Denmark, University of Copenhagen, Universitetsparken 15, DK-2100 Copenhagen Ø, Denmark. [52]Bell Museum of Natural History, University of Minnesota, Saint Paul, MN 55108, USA. [53]Department of Life Sciences, Natural History Museum, Cromwell Road, London SW7 5BD, UK. [54]Department of Life Sciences, Imperial College London, Silwood Park Campus, Ascot SL5 7PY, UK. [55]Smithsonian Conservation Biology Institute, National Zoological Park, Front Royal, VA 22630, USA. [56]Smithsonian Conservation Biology Institute, National Zoological Park, Washington, DC 20008, USA. [57]Theodosius Dobzhansky Center for Genome Bioinformatics, St. Petersburg State University, St. Petersburg, Russia 199004. [58]Oceanographic Center, Nova Southeastern University, Ft Lauderdale, FL 33004, USA. [59]Center for Biomolecular Science and Engineering, UCSC, Santa Cruz, CA 95064, USA. [60]San Diego Zoo Institute for Conservation Research, Escondido, CA 92027, USA. [61]Department of Vertebrate Zoology, MRC-116, National Museum of Natural History, Smithsonian Institution, Washington, DC 20013, USA. [62]Department of Environmental Health Science, University of Georgia, Athens, GA 30602, USA. [63]Moore Laboratory of Zoology and Department of Biology, Occidental College, Los Angeles, CA 90041, USA. [64]Department of Genomics and Genetics, The Roslin Institute and Royal (Dick) School of Veterinary Studies, University of Edinburgh, Easter Bush Campus, Midlothian EH25 9RG, UK. [65]Swedish Species Information Centre, Swedish University of Agricultural Sciences Box 7007, SE-750 07 Uppsala, Sweden. [66]Key Laboratory of Zoological Systematics and Evolution, Institute of Zoology, Chinese Academy of Sciences, Beijing 100101, China. [67]Department of Organismic and Evolutionary Biology and Museum of Comparative Zoology, Harvard University, Cambridge, MA 02138, USA. [68]Institute of Theoretical Informatics, Department of Informatics, Karlsruhe Institute of Technology, D- 76131 Karlsruhe, Germany. [69]Department of Biochemistry and Biophysics, University of California, San Francisco, CA 94158, USA. [70]Department of Ornithology, American Museum of Natural History, New York, NY 10024, USA. [71]Department of Biology and Genetics Institute, University of Florida, Gainesville, FL 32611, USA. [72]Departments of Bioengineering and Computer Science, University of Illinois at Urbana-Champaign, Urbana, IL 61801, USA. [73]Department of Biology, University of Copenhagen, Ole Maaløes Vej 5, 2200 Copenhagen, Denmark. [74]Princess Al Jawhara Center of Excellence in the Research of Hereditary Disorders, King Abdulaziz University, Jeddah 21589, Saudi Arabia. [75]Macau University of Science and Technology, Avenida Wai long, Taipa, Macau 999078, China. [76]Department of Medicine, University of Hong Kong, Hong Kong. [77]Centre for Social Evolution, Department of Biology, Universitetsparken 15, University of Copenhagen, DK-2100 Copenhagen, Denmark.

*These authors contributed equally to this work. †Corresponding author. E-mail: jarvis@neuro.duke.edu (E.D.J.); tandywarnow@gmail.com (T.W.); mtpgilbert@gmail.com (M.T.P.G.); wangj@genomics.cn (W.J.); zhanggj@genomics.cn (G. Z.)

for estimating species trees from genome-scale concatenated sequence alignments (SM4) (*55–57*). We also developed a statistical binning approach that improves multispecies coalescent analyses for handling gene trees with low phylogenetic signal to infer a species tree (SM5) (*58*). These computationally intensive analyses were conducted on more than 9 supercomputer centers and required the equivalent of >400 years of computing using a single processor (SM3 and SM4).

From these efforts, we identified a high-quality orthologous gene set across avian species, consisting of exons from 8251 syntenic protein-coding genes (~40% of the proteome), introns from 2516 of these genes, and a nonoverlapping set of 3769 ultraconserved elements (UCEs) with ~1000 bp of flanking sequences. This total evidence nucleotide data set comprised ~41.8 million bp (table S3 and SM4), representing ~3.5% of an average avian genome.

A genome-scale avian phylogeny

Total evidence nucleotide tree

The total evidence nucleotide alignment partitioned by data type (introns, UCEs, and first and second exon codon positions; third positions excluded as described later) analyzed with ExaML under the GTR+GAMMA model of sequence evolution (SM4) resulted in a highly resolved total evidence nucleotide tree (TENT) (Fig. 1 and fig.

S1). The three recognized major groupings within extant birds—Palaeognathae, Galloanseres, and Neoaves (the latter two united in the infraclass Neognathae)—were recovered with full (100%) bootstrap support (BS). The tree revealed the first divergence within extant Neoaves, resulting in two fully supported, reciprocally monophyletic sister clades that we named Passerea (after its most speciose group Passeriformes) and Columbea (after its most speciose group Columbiformes) (Fig. 1; see SM6 for rationale of clade names).

Within Passerea, the TENT strongly confirmed the monophyly of two large closely related clades that we refer to as core landbirds (Telluraves) and core waterbirds (Aequornithia) (*8, 16, 17, 27, 36, 59*);

Fig. 1. Genome-scale phylogeny of birds. The dated TENT inferred with ExaML. Branch colors denote well-supported clades in this and other analyses. All BS values are 100% except where noted. Names on branches denote orders (-iformes) and English group terms (in parentheses); drawings are of the specific species sequenced (names in table S1 and fig. S1). Order names are according to (*36, 37*) (SM6). To the right are superorder (-imorphae) and higher unranked names. In some groups, more than one species was sequenced, and these branches have been collapsed (noncollapsed version in fig. S1). Text color denotes groups of species with broadly shared traits, whether by homology or convergence. The arrow indicates the K-Pg boundary at 66 Ma, with the Cretaceous period shaded at left. The gray dashed line represents the approximate end time (50 Ma) by which nearly all neoavian orders diverged. Horizontal gray bars on each node indicate the 95% credible interval of divergence time in millions of years.
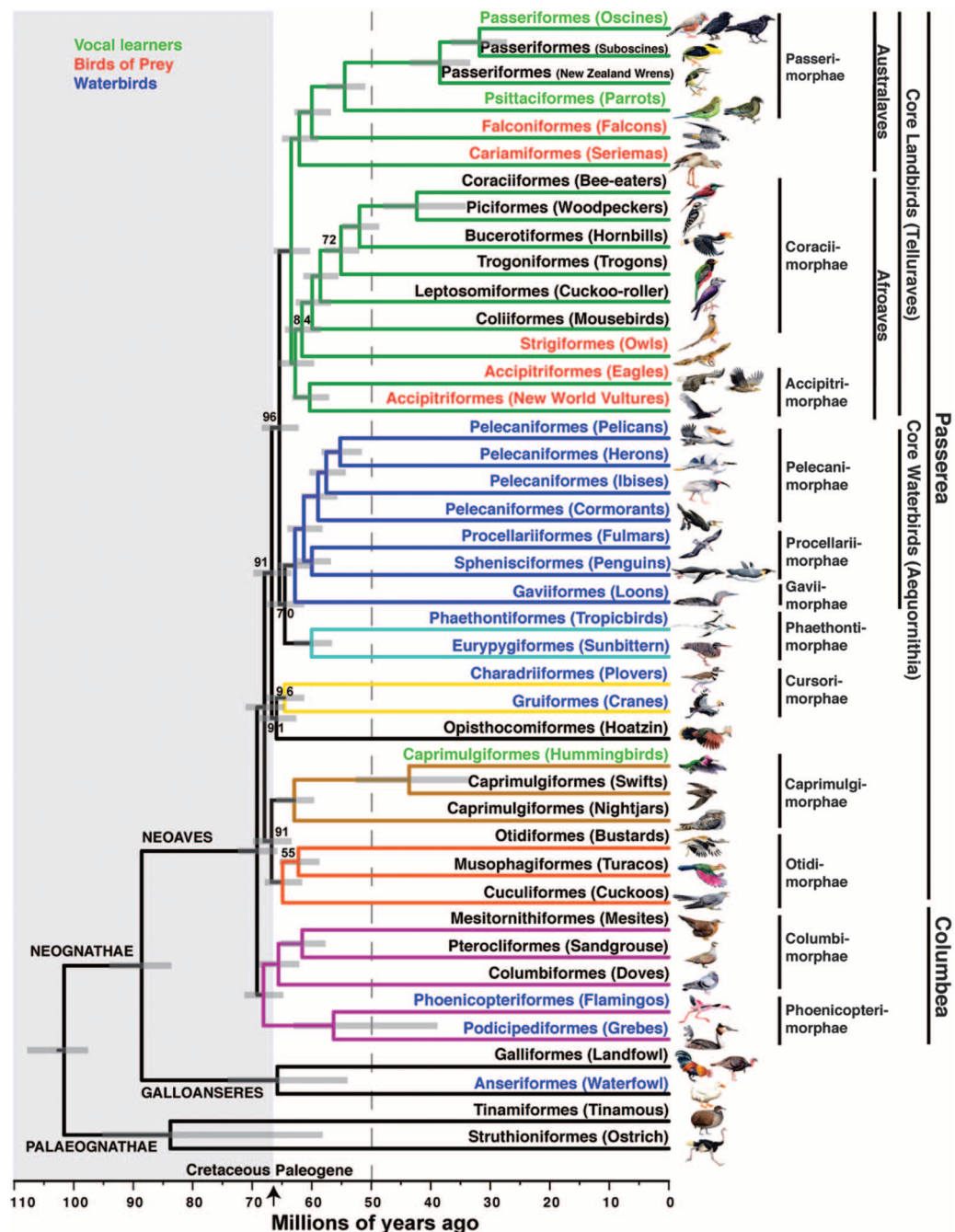
we use the term "core" instead of "higher" to prevent interpretation that these groups are more advanced or more recently evolved than other birds. Within core landbirds, we found 100% BS for a previously more weakly supported clade (Australaves) containing seriemas (historically placed in Gruiformes), falcons (historically grouped with other diurnal birds of prey), parrots (historically difficult to place), and Passeriformes and a sister clade (Afroaves) containing Accipitrimorphae birds of prey, owls, mousebirds, woodpeckers, and bee eaters, among others (Fig. 1) (*8*, *17*, *26*, *29*, *60*).

Core waterbirds were sister to a fully supported clade (Phaethontimorphae) containing tropicbirds and the sunbittern (Fig. 1) (*27*, *28*). We did not include Phaethontimorphae in the core waterbirds because their relationship had relatively low 70% BS, although their aquatic (tropicbirds)
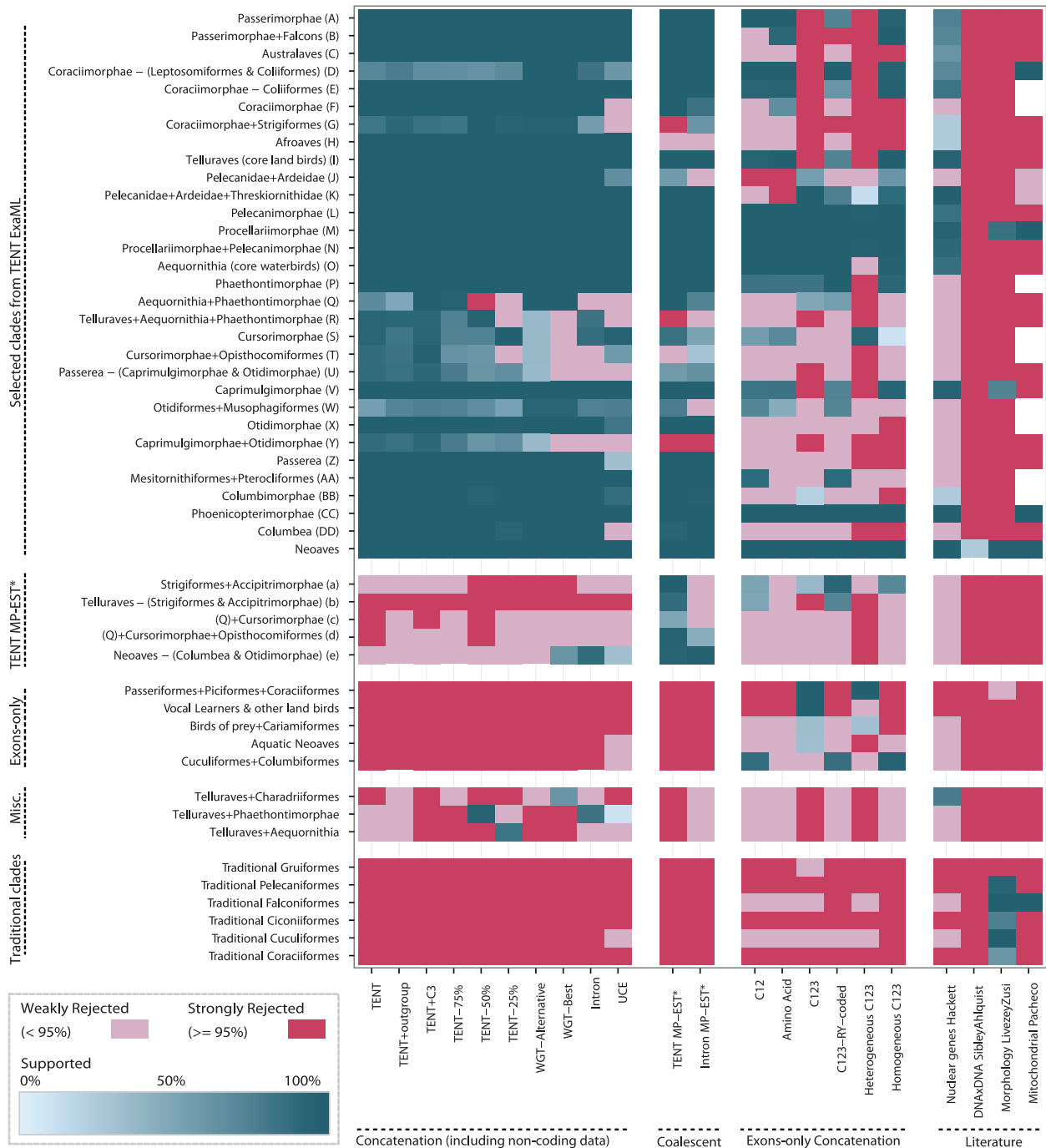
Fig. 2. Metatable analysis of species trees. Results for different genomic partitions, methods, and data types are consistent with or contradict clades in our TENT ExaML, TENT MP-EST*, and exon-only trees and previous studies of morphology (*15*), DNA-DNA hybridization (*24*), mitochondrial genes (*14*), and nuclear genes (*17*). Letters (A to DD and a to e) denote clade nodes highlighted in Fig. 3, A and B, of the ExaML and MP-EST* TENT trees. Each column represents a species tree; each row represents a potential clade. Blue-green signifies the monophyly of a clade, and shades show the level of its BS (0 to 100%). Red, rejection of a clade; white, missing data. We used a 95% cut-off (instead of a standard 75%) for strong rejection due to higher support values with genome-scale data. The threshold for the mitochondrial study was set to 99% due to Bayesian posterior probabilities yielding higher values than BS. An expanded metatable showing partitioned ExaML, unbinned MP-EST, and additional codon tree analyses is shown in fig. S2.

and semiaquatic (sunbittern) lifestyles are consistent with a waterbird grouping, and multiple analyses presented below group them with 100% BS. The TENT also resolved at 100% BS taxa that were previously difficult to place, including uniting cuckoos, turacos, and bustards (Otidimorphae) and placement of the mousebird among core landbirds. The Columbea also had separate landbird and waterbird groups. These results demonstrate that genome-scale data can help resolve difficult relationships in the tree of life.

Comparisons of TENT with previous studies

The TENT contradicted some relationships in avian phylogenies generated from morphological characters (*15*), DNA-DNA hybridization (*24*), and mitochondrial genomes (*14, 18*) (Figs. 2, figs. S2, and Fig. 3A versus fig. S3, A to C). For example, our Falconiformes excluded the previously included eagles and New World vultures (now in Accipitrimorphae); our Coraciiformes was more narrowly delineated and excluded hornbills and cuckoo-rollers; our Pelecaniformes excluded tropicbirds; and our Gruiformes excluded seriemas, bustards, the sunbittern, and mesites. The TENT did not fully support the view based on one gene (*β-fibrinogen*) that the first divergence in Neoaves resulted in two equally large Metaves and Coronaves radiations (*25*). However, all Columbea species in the TENT were in the previously defined Metaves, supporting the hypothesis of two parallel radiations of birds with convergent adaptations (*25*).

The TENT was most congruent with past (*8, 17*) and more recent (*27, 28*) smaller-scale multilocus nuclear trees (Figs. 2 and 3A and fig. S3D), although most congruence was limited to the core landbirds and core waterbirds. Within the former, we recovered Australaves and Afroaves (*60*), although with a different branching ordering in our tree; our taxon sampling is insufficient to address the biogeographic justification of their names. The TENT recovered a number of groups not present in these previous trees, and even for those present, the TENT had higher BS (Fig. 2). Absence of nonavian outgroups in our TENT above was not responsible for variation with past studies because we recovered the same topology when including outgroups (Fig. 2 and fig. S4, A and B), despite the outgroups having only ~30% orthologous sequences in the TENT alignment (e.g., fig. S21; SM3).

More data are responsible for resolving early branches of the tree

Despite the many fully supported (100% BS) relationships in the TENT, lower support was obtained for 9 of the 45 internal branches (although still within the high 70 to 96% BS range). Almost all were at deep divergences within the Neoaves, after the Columbea and Passerea divergence and before the ordinal divergences (Fig. 1 and fig. S1). The monophyly of each of the superorders, however, had 100% BS. The presence of these lower BS values is in contrast to the expectation that genome-scale alignments would result in complete phylogenetic resolution (*34, 35, 61*).

However, consistent with this hypothesis, we found that most relationships that had less than 100% BS with the full TENT data exhibited a steady increase in support with an increase in random subsets of the TENT data (Fig. 2 and fig. S5). The placement of the Phaethontimorphae (sunbittern and tropicbirds) and hoatzin changed when smaller (25 to 50%) amounts of data were analyzed. Further exploring data amount, we used the assembled ~1.1-billion-bp chicken genome (*40*) as a reference to generate a 322-million-bp MULTIZ alignment of putatively orthologous genome regions across all species, comprising ~30% of an average assembled avian genome and corresponding to the maximal orthologous sequence obtainable across all orders under our homology criteria (SM3). We ran ExaML on the alignment for ~42 CPU years, with 20 maximum likelihood searches on distinct starting trees and 50 bootstrap replicates before reaching our convergence criterion (SM4) on a whole-genome tree (WGT). Notably, all runs resulted in one of two trees: one identical to the TENT topology (fig. S4C) and a second almost identical to the TENT (fig. S4D). This latter tree differed from the TENT by local shifts in five branches, all clades that had less than 100% BS in the TENT (fig. S4, A and D). Given the relatively minor differences between the second WGT and the TENT, together they corroborate the majority of relationships in the avian tree of life. Although the WGT has more data (table S3), the orthology (SM2) and alignment (SM3) qualities are higher for the TENT, and thus we consider the TENT more reliable.

Noncoding data contribute more to the TENT topology

We sought to determine if different genomic partitions contribute differently to the TENT and found that ExaML trees using only introns or UCEs from the TENT data were largely congruent with the TENT and WGTs for branches that had strong support (BS > 75%) in the intron and UCE trees (Figs. 2; 4, A and B; and 5B). However, the intron tree, and even more so the UCE tree, had lower resolution than the TENT (Fig. 5A), mostly on deep branches (Fig. 4, A and B), consistent with fewer data leading to lower resolution on deeper branches. For the intron tree, some lower-resolution branches had local shifts, but they matched those found in the second WGT or the 25 to 75% data subsets of the TENT; an exception was Phaethontimorphae, which moved from being sister to core waterbirds with 70% BS in the TENT (but 100% BS in the WGTs) to sister to core landbirds with 86% BS in the intron tree. For the UCE tree, the lower-resolution, deep branches had more distant shifts. Trees created from analysis of the first and second codon positions (exon c12) of the TENT data also had lower levels of BS (~39 to 64%) but with more topological differences on the deep branches (Figs. 2, 4C, and 5A), yet all but one of the fully resolved relationships (local difference in egret + ibis + pelican) were congruent with the TENT (Fig. 5B).

These findings demonstrate that noncoding intron sequences lend greater support for the TENT than the protein-coding and UCE sequences, con-

sistent with intron sequences having a higher rate of evolution (SM4) and thus greater phylogenetic signal. These differences are not merely due to shorter alignments of the exon and UCE sequences, because each accounted for ~25% of the TENT data, similar in sequence length to the random 25% subset of the TENT with introns (table S3) that produced a tree with a higher average BS and a topology closer to the full TENT (Fig. 5A and fig. S5D).

Incomplete lineage sorting and impact on deep branches

Deeper branches exhibit higher gene tree incongruence

We next investigated ILS, a population-level process that results in incongruence between gene trees and the species tree (*62*). Consistent with conditions that could lead to ILS (*63*), the TENT had a wall of many (25 of 45; ~55%) very short internal branches (0.0006 to 0.002 substitutions per site), almost all at deep divergences within Neoaves (Fig. 3A, inset, and fig. S7). Indeed, all nine branches with <100% BS were among the shortest in the TENT (fig. S8), many in succession, suggesting that reduced BS could be related to conflict among gene trees.

To test this hypothesis, we compared the distribution of gene trees that have strong conflict (>75% BS) with branches of the ExaML TENT. We focused on introns because they had greater gene tree resolution (higher average BS) than exons or UCEs (fig. S24 and SM4). The 2485 introns with orthologs available in the two outgroup Palaeognathae species ranged from exhibiting no conflict to exhibiting considerable conflict (up to 950 genes or 38%) for some branches of the TENT (Fig. 3A, blue numbers, and Fig. 5C). The percentage of gene tree conflict was successively higher for the shorter and deeper branches of the TENT (Fig. 3A), particularly those with <100% BS (e.g., branches R, U, and Z in Fig. 3, A and C). Conversely, these short branches had fewer (0 to 20%) intron gene trees supporting them at high (>75%) BS levels (Fig. 3A, black numbers, and Fig. 3D). These findings suggest that ILS could have affected the inferred relationships of some of the deep branches of Neoaves in the concatenated tree analysis.

Multispecies coalescent approach infers a species tree similar to the TENT

To determine if ILS affected the concatenated tree analyses, we explored whether a multispecies coalescent model leads to a different tree topology. Multispecies coalescent methods estimate the species tree from a set of gene trees and are statistically consistent when discordance among gene trees results from ILS (*64, 65*). However, the inferred species tree can have low resolution (BS) and be less topologically accurate when the input gene trees are poorly resolved (*33, 66*), a problem that many of our genes faced (SM4). Thus, we developed a statistical binning technique that first groups genes into sets based on phylogenetic similarities, from each set estimates a supergene tree, and uses them in the maximum pseudolikelihood estimation of the species tree

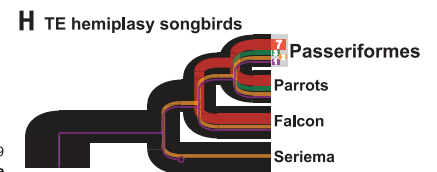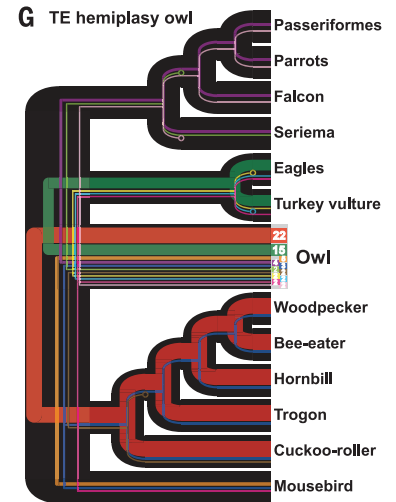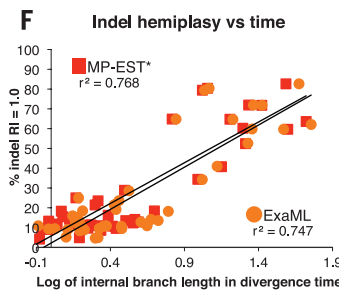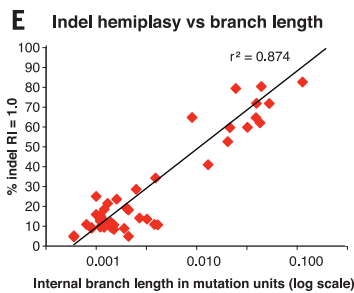(MP-EST) multispecies coalescent approach (*67*) to infer a species tree (SM5) (*58*).
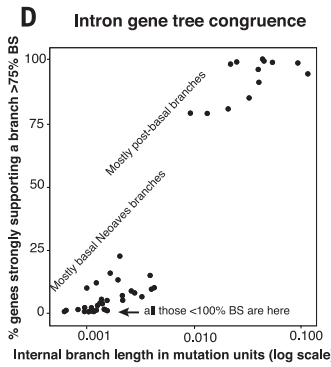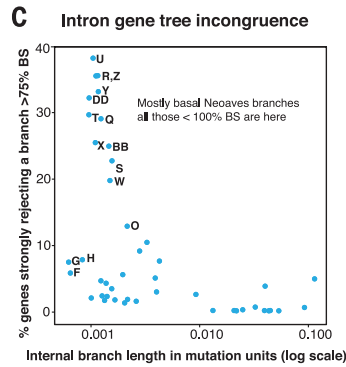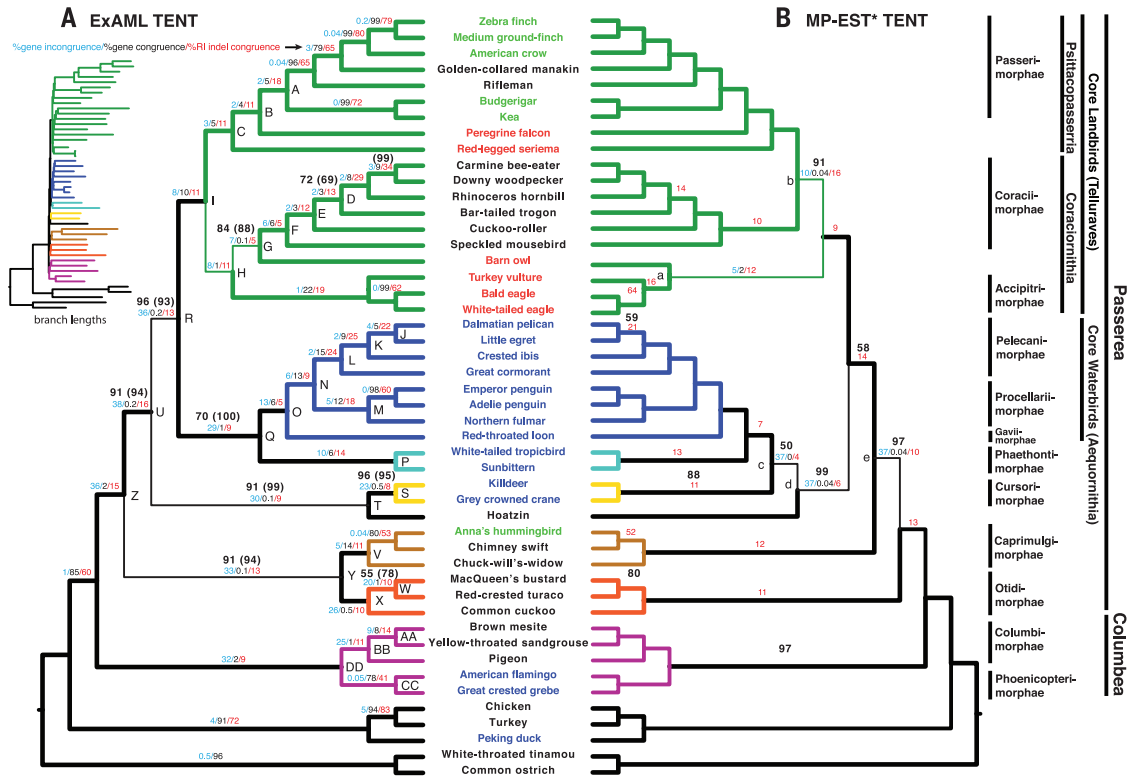
This approach produced more accurate estimated species trees compared with MP-EST applied to unbinned gene data sets that have low phylogenetic signal (i.e., figs. S2 and S9; SM7) (*58*). It produced a highly resolved binned MP-EST (MP-EST*) TENT tree that was highly congruent with the ExaML TENT (Fig. 3, A and B). There were only local shifts of five clades, nearly all on lower-support (<100% BS) branches of the ExaML and MP-EST* TENTs (Fig. 3, A and B). The monophyly of Afroaves was the only case of 100% BS in the ExaML TENT that conflicted with the MP-EST* TENT tree and involved a local shift in

Fig. 3. Evidence of ILS.
(**A**) Cladogram of ExaML TENT avian species tree, annotated for nodes from Fig. 2 (letters), for branches with less than 100% BS without and with (parentheses) third codon positions, for strong (>75% BS) intron gene tree incongruence and congruence, and for indel congruence on all branches (except the root). Thin branch lines represent those not present in the MP-EST* TENT of (B). (Inset) ExaML branch lengths in substitution units (expanded view in fig. S7). Color coding of branches and species is as in Fig. 1. (**B**) Cladogram of MP-EST* TENT species tree, annotated similarly as in the ExaML TENT in (A). Thin branch lines represent those not present in the ExaML TENT of (A). (**C**) Percent of intron gene trees rejecting (≥75% BS) branches in the ExaML TENT species tree relative to branch lengths. Letters denote nodes in (A) that either have less than 100% support or are different from the MP-EST* TENT in (B). (**D**) Percent of intron gene trees supporting (≥75% BS) branches in the ExaML TENT species tree relative to branch lengths. (**E**) Indel hemiplasy [the inverse of percent of retention index (RI) = 1.0 indels that support the branch; see SM9] correlated with ExaML TENT branch length (log transformed). r^2, correlation coefficient. (**F**) Indel hemiplasy correlated with ExaML and MP-EST TENT internal branch divergence times in millions of years (log transformed). Plotting with internal branch times was necessary to compare both trees (SM9). (**G**) TE hemiplasy with owls among the core landbirds. Line color, shared TE tree topology; line thickness, relative proportion of TEs that support a specific topology (total numbers shown in the owl node). Circles at end of lines indicate loss of the TE allele in that species after ILS, as the sequence assembly contains an empty TE insertion site (SM10). Only topologies with two or more TEs are shown. (**H**) TE hemiplasy with songbirds among the core landbirds.
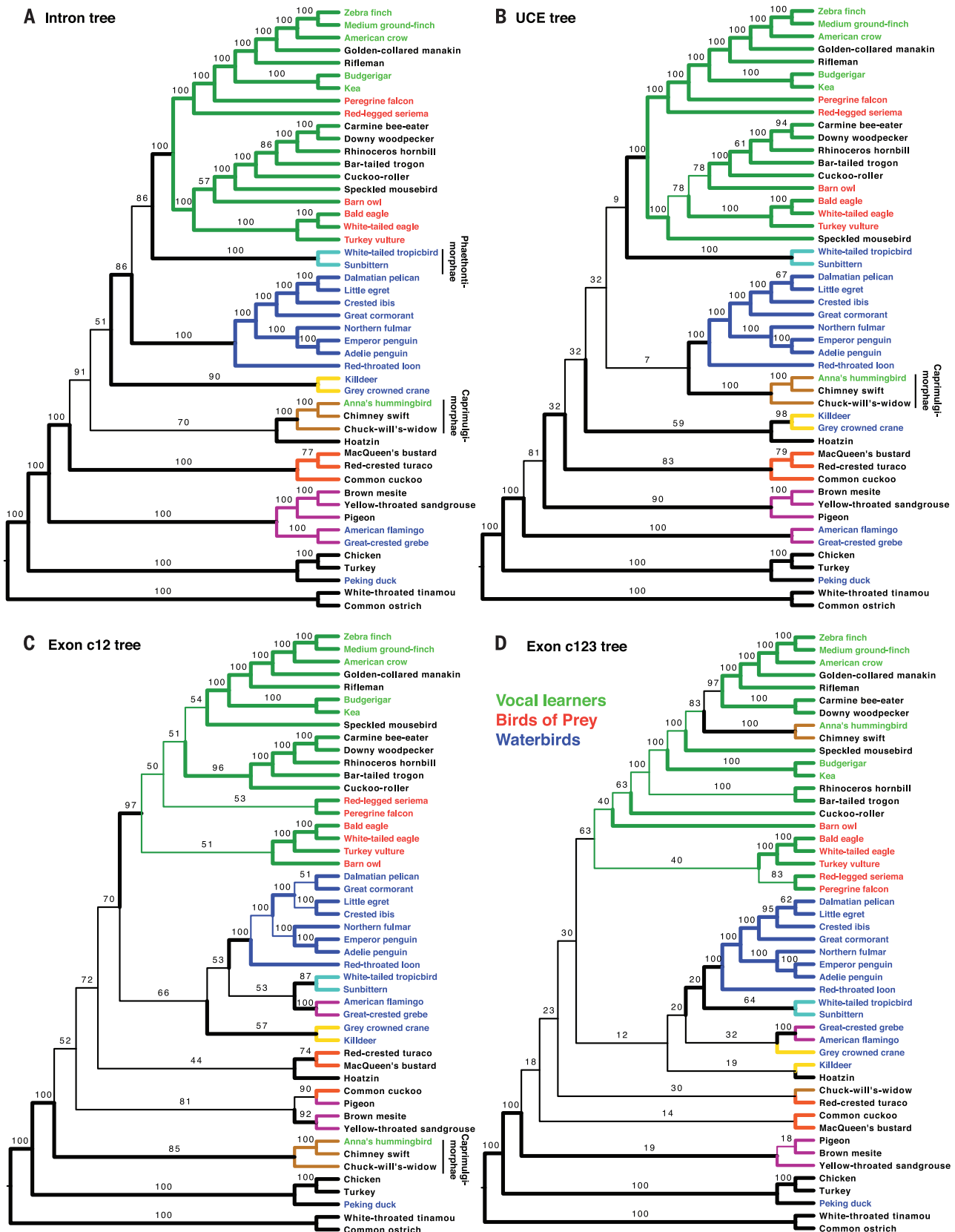
Fig. 4. Species trees inferred from concatenation of different genomic partitions. (**A**) Intron tree. (**B**) UCE tree. (**C**) Exon c12 tree. (**D**) Exon c123 tree. The tree with the highest likelihood for each ExaML analysis is shown. Color coding of branches and species is as in Fig. 1 and fig. S1. Thick branches denote those present in the ExaML TENT. Numbers give the percent of BS.
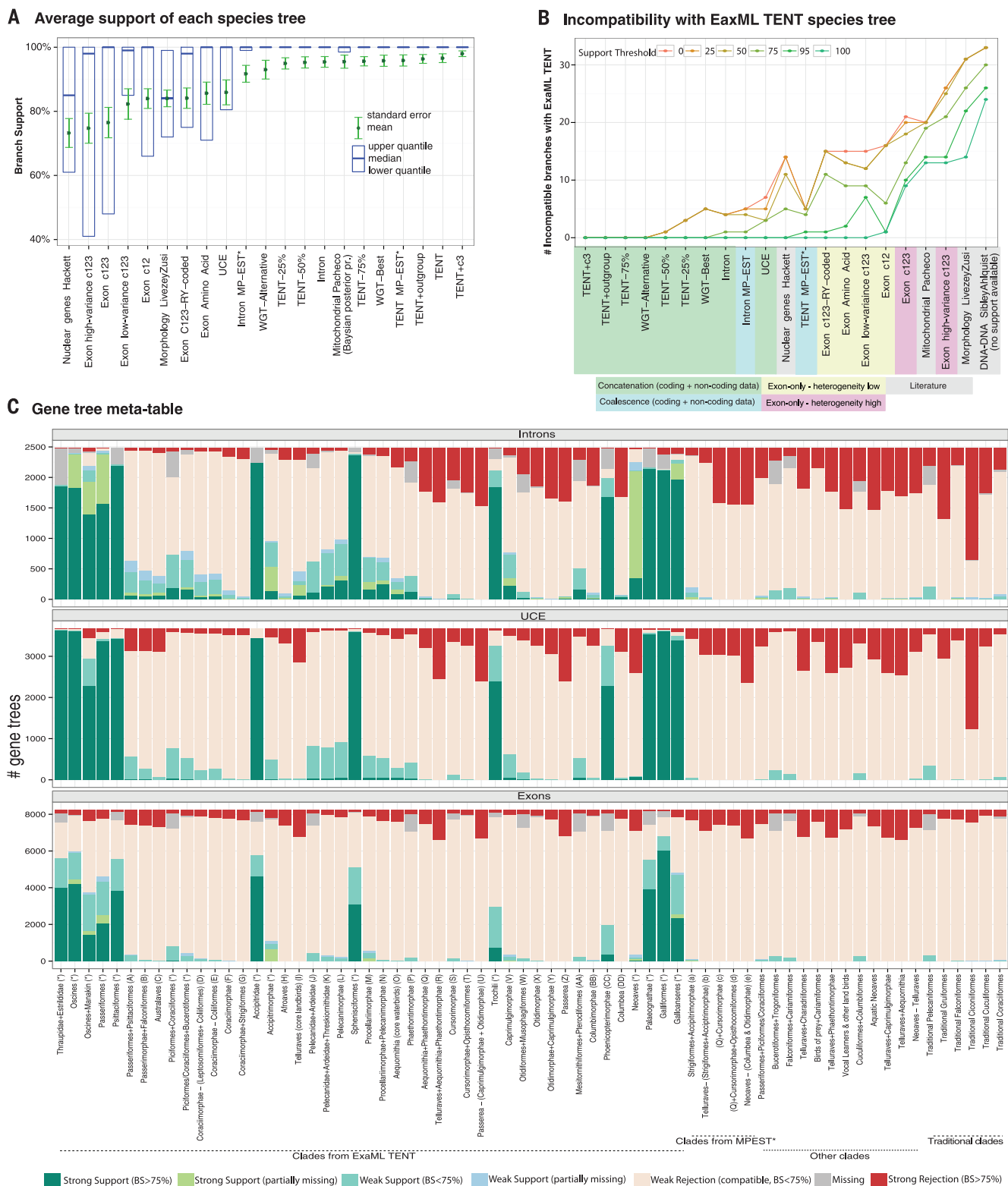
Fig. 5. Comparisons of total support among species trees and gene trees. (**A**) Average BS across all branches of species trees from varying input data as in Fig. 2, ordered left to right from lowest to highest values. (**B**) Numbers of incompatible branches (out of 45 internal), at different support thresholds, with the ExaML TENT tree, ordered left to right from most to least compatible (expanded analysis in fig. S6). (**C**) Analyses of intron, exon, and UCE gene tree congruence and incongruence with nodes

in the ExaML TENT, MP-EST* TENT, and other species trees. Names and letters for clades are as in Figs. 2 and 3. "Missing" denotes the case in which an ortholog is not present for any taxa or is present for only one taxon, and hence monophyly cannot be determined. "Partially missing" indicates the case in which some taxa are missing but at least two of the taxa are present, and thus we can still categorize it as either monophyletic or not. For further details, see SM7.

the owl with mousebirds and Accipitrimorphae birds of prey. Two branches with <100% BS in the ExaML TENT increased to 100% in the MP-EST* TENT, including Phaethontimorphae with core waterbirds. The intron trees supported some branches more in the ExaML and some more in the MP-EST* TENT (Fig. 3, A and B). Nevertheless, the overall topology of both trees was very similar, including the basal Columbea and Passerea divergence.

All estimates of gene trees differ from our candidate species trees

No single intron, exon, or UCE locus from our TENT data set had an estimated topology identical to the ExaML TENT or MP-EST* TENT (fig. S10, A and B). The top three loci (all introns) with the closest inferred topologies differed from the two versions of the TENT on more than 20 to 30% of their branches. Average topological distance with the ExaML species tree was 63% for the introns, 66% for the UCEs, and 80% for the exons. To test whether our total evidence data set missed some genes with the TENT topologies, we constructed a more comprehensive collection of genes trees with phylomeDB, which assigns orthology using maximum likelihood analyses (http://phylomedb.org) [see SM8 and (68)]. For ~13,000 (low-coverage genomes) to ~18,000 (high-coverage genomes) annotated genes across avian species (44), phylomeDB inferred orthologs for 94.58% of them and these agreed with the synteny-based orthology of the 8251 protein-coding genes of the TENT by 93%. This more complete set of protein-coding genes still did not have a single estimated gene tree that was fully congruent with the ExaML or MP-EST* TENT trees (fig. S10, C and D), and there was overall low congruence with the species trees (http://tol.cgenomics.org/birds_v1) (fig. S11, A and B). The conflicting nodes largely reflected branches with low statistical support (approximate likelihood ratio test < 0.95), which primarily corresponded to the short successive deep branches of Neoaves. These findings can be explained by both a low amount of phylogenetic signal in individual loci (figs. S24 to S26 and SM4) and a high amount of ILS during the neoavian radiation.

Indels suggest a high degree of ILS at the earliest branches of the Neoaves tree

We further assessed ILS using insertions and deletions (indels) (69), because they have less homoplasy (convergence) than single nucleotides (SM9), and unlike gene trees, indels can be examined as discrete characters mapped to a reference tree without the added inference of constructing trees from them. We scored 5.7 million indels from the TENT alignment, of which 24% were shared by two or more taxa (table S3). We found indel incongruence on all branches of the ExaML TENT, as measured inversely by the percent of the indel characters uniquely defining each branch (Fig. 3A, red numbers; SM9). Like the gene trees, there appeared to be a successive decrease in the percentage of indels that supported deeper branches of each major clade (Fig. 3A). Most branches with

the highest levels of indel incongruence belonged to the shortest and deepest ones that made local shifts in analyses, with the two branches joining mousebirds and owls exhibiting the highest indel incongruence and the shortest internal branch lengths in the ExaML TENT (Fig. 3A and fig. S7). Consistent with these findings, indel incongruence was inversely correlated with internal branch length, and branch length explained 87% (r^2) of the variation in the percentage of nonhomoplasious indels defining each branch (Fig. 3E). The correlation of indel incongruence versus branch time was similar for both ExaML and MP-EST* TENT trees (Fig. 3F).

Indel incongruence is not due to the indels supporting another species tree, as applying ExaML on indels from the total evidence alignment as binary data produced a total evidence indel tree that was largely congruent with the ExaML TENT and MP-EST* TENT for all but one node with a local shift of pigeon within Columbea (fig. S12). Homoplasy due to convergence is thought to be positively correlated with branch length [i.e., long branch attraction (70)]. The only known source of incongruence that is inversely correlated with internal branch length is hemiplasy (differential inheritance of polymorphic alleles) (64, 71). Because hemiplasy is a hallmark of ILS and 87% of the variation in indel incongruence is explained by branch length, our indel findings suggest high levels of ILS during the basal radiation of Neoaves, with comparable support for the ExaML or MP-EST* versions of the TENT.

Transposable elements with higher ILS in the deepest branch of core landbirds with owls

We tested for a signature of ILS in TE insertions, which have extremely low homoplasy because independent insertions into the same location in a genome are rare (SM10) (72, 73). We focused on the owl because its position exhibited one of the strongest incongruencies among the species tree results. Of 3671 barn owl long terminal repeat TE insertion loci orthologous in all of the bird genomes, 61 were informative for owls among core landbirds and showed two dominant exclusive TE topologies: (i) an owl + Accipitrimorphae topology, as seen in the MP-EST* TENT; and (ii) an owl + Coraciimorphae topology that excludes mousebird, as seen in the UCE tree (Fig. 3G compared to Figs. 3B and 4B). Nine other topologies had fewer markers supporting them. In contrast, for 25 informative TEs of Neoaves in (29), 13 were informative for Australaves, and of these, 3 were exclusive for Passeriformes + parrots, 7 for Passeriformes + parrots + falcons, and 2 for the latter group plus seriemas, with no alternative topologies for the first two groups (Fig. 3H). If the passeriform TE insertions exhibited a similar mixture of alternative distributions as for the owl, just 10 markers would result in conflicting distributions (4 with one, 3 with another, and 3 for the remaining topologies) instead of a conflict-free topology. Although this analysis is limited to specific taxa, it suggests higher ILS near the deepest branches of Afroaves involving the owl, consistent with the branch length, gene tree, and indel findings.

Overall, these results reveal considerable ILS during the neoavian radiation and that, even with genome-scale data, ILS may affect the inference of small local relationships in the deep branches of the species tree that have long been more challenging to resolve. However, ILS does not affect the majority of other phylogenetic relationships we found using genome-scale data.

Protein-coding data resolve avian phylogeny poorly but reflect life history traits

Codon positions of protein-coding genes and life history relationships

We investigated sources of lower resolution and incongruence for the tree based on protein-coding sequences (Fig. 4C). This is crucial for phylogenomic inference, as many studies [including transcriptome analyses (19, 74)] use only protein-coding genes to infer species trees. We found that ExaML analyses with either all (c123; Fig. 4D) or individual codon positions (c1, c2, c3; fig. S13, A to C) produced trees with lower BS (Fig. 5A) and greater differences in topologies (Fig. 2 and fig. S2) compared with noncoding data and coding + noncoding combined. The differences between coding versus noncoding trees were not solely due to shorter sequence length of the coding data, because the full coding data set (13.3 million bp for c123) produced a tree with fully supported (100% BS) relationships that were incongruent with those fully supported in the intron (19.3 million bp), TENT (37.4 million bp without the third codon position), and WGT (322.1 million bp) (Figs. 2 and 5B, and table S3). Surprisingly, the c123 topology associated species more with life history traits than the TENT topology. This included a strongly supported clade (100% BS on most branches) that comprised the three groups of vocal learners (parrots, songbirds, and hummingbirds) and most of the nonpredatory core landbirds, a monophyletic clade of diurnal birds of prey and seriemas (albeit with low 40% BS), and a monophyletic clade of all aquatic and semiaquatic species of Passerea and Columbea (also with low 20% BS) (Fig. 4D). Partitioning the data to account for possible differences in evolutionary rates among genes (SM4) did not result in a tree more similar to the TENT, but instead in a tree with increased support for monophyletic groupings of species with these broadly shared traits (fig. S14C). The c1, c2, and amino acid tree topologies (fig. S13, A, B, and D) were more congruent with the c12 tree (Figs. 2 and 4C), consistent with these two codon positions largely specifying amino acid identity. In contrast, the c3 tree was very similar to the c123 tree but with higher BS (63 to 82%) for similar trait groupings; it moreover brought all basal neoavian landbirds together as sister to all neoavian aquatic/semiaquatic species (figs. S2 and S13C). Most individual gene trees show weak to strong rejection of these relationships (Fig. 5C).

As expected (19), the third codon position exhibited greater base composition variation among species than the other codon positions and even other genomic partitions (fig. S15A). Although all codon positions violated the stationarity assumption

in the GTR + GAMMA model of sequence evolution, the third codon position exhibited a much stronger violation (fig. S15B). Reducing this variation by RY recoding of purines (R) and pyrimidines (Y) on the third codon position (SM4) made the c123 tree topology more similar to the c12 topology (Fig. 2 and fig. S14D). These results demonstrate that the third codon position exerts a strong influence on the protein-coding–tree topology, overriding signals from the first and second codon positions. They also suggest that a signal in the third codon position could also be associated with convergent life history traits.

Heterogeneous protein-coding genes associated with life history traits

We further investigated the source of the conflict in the protein-coding genes (SM11) and found that trees using all codon positions from the 10% most compositionally homogeneous (low-variance) exons (n = 830) were most congruent with the c12 tree and, thus, more similar to the TENT than to the c123 tree (Figs. 2 and 6A; cladograms in fig. S16, A to C). Conversely, trees using all codon positions from the 10% most compositionally heterogeneous (high-variance) genes (n = 830) were more congruent with the exon c123 and c3 trees (Figs. 2 and 6B and fig. S16, B and D). The branch lengths of the high-variance exon tree showed a strong positive correlation with GC content and a negative correlation with the average body mass of species, seen at a much lesser magnitude in the low-variance exon tree (Fig. 6, A to D). The correlations for the high-variance genes were also strongest on the third codon position (fig. S17, A and B) (75, 76). In addition, the genomic positions of the high-variance genes were skewed toward the ends of the chromosomes, whereas the positions of the low-variance genes were skewed toward the center (Fig. 6, E and F, and fig. S17, C and D). Although the available introns of these genes had significant correlations among GC content and body mass and among GC content and chromosome position, they exhibited less heterogeneity overall (fig. S17, A to D) and yielded trees that were much more congruent with each other and with the TENT (figs. S2 and S17, E and F). An ExaML TENT tree that included the third codon position (TENT + c3) was identical in topology to the ExaML TENT without the third codon position and had increased support for six of the nine branches that had less than 100% BS (fig. S1 versus fig. S18, also Figs. 3A and 5A).

These results suggest that in the context of protein-coding data only, high–base compositional heterogeneity and life history have a strong impact on incongruence with the species tree, and thus are not suitable for generating a highly resolved phylogeny. However, in the context of large amounts of noncoding genomic data, the phylogenomic signal in the exon data adds support to the species tree.

Dating the radiation of Neoaves

The generation of a well-resolved avian phylogeny allowed us to address the timing of avian diversification. To estimate the avian timetree with genomic-scale data, we used first and second codon positions from 1156 clock-like exon genes (which do not strongly exhibit the above protein-coding compositional bias), calibrated with 19 conservatively chosen avian fossils (plus nonavian outgroups) as minimum bounds for lineage ages (with a maximum-bound age constraint of 99.6 Ma for Neornithes), in a Bayesian autocorrelated relaxed clock method using MCMCTREE (77) on the fixed ExaML TENT topology (SM12).

Our results suggest that after the Palaeognathae and Neognathae divergence about 100 Ma in the Late Cretaceous, the Palaeognathae diverged into their two stem lineages [ostrich and tinamous (11, 78)] about 84 Ma, and the Neognathae diverged into their stem lineages (Galloanseres and Neoaves) about 88 Ma (Fig. 1). Although the 95% credibility interval for the ostrich-tinamou divergence is broad, its lower bound is consistent with the fossil record (79). In contrast, both the earliest divergence within Galloanseres and an explosive diversification within Neoaves were dated to occur around the K-Pg boundary, with 95% credibility intervals spanning 6.5 million years, on average. In particular, the most basal divergences within Neoaves (Columbea, Passerea, and two more) occurred before the K-Pg transition (67 to 69 Ma) and all others after, with nearly all ordinal divergences completed by 50 Ma (Fig. 1, dashed line). The estimated age for the basal split of Passeriformes, representing ~60% of all living ~10,400 avian species, was around 39 Ma. These divergence times conflict with some previous studies based on nuclear (9–12) and mitochondrial (13, 14) DNA but are consistent with the fossil record (80), including the identification of *Vegavis iaai*, a very Late Cretaceous (66 to 68 Ma) stem-anseriform fossil (80, 81), and the dearth of verifiable Neoaves fossils in the Late Cretaceous (5). These findings were similar regardless of the specific tree from this study we dated or whether we used a later minimum age (86.5 Ma) for Neornithes (table S16; more discussion on dating in SM12).

Discussion

Our study is an example of the extraordinary amount of genomic sequence data required to produce a highly supported phylogeny spanning a rapid radiation. The conflict we observe with other data types (14, 15, 24) can no longer be considered to be due to error from smaller amounts of sequence data (8, 17) nor to differences in concatenation versus coalescence methods (27, 28). The absence of a single gene tree identical to the avian species tree is consistent with studies in yeast (82), indicating that phylogenetic studies based on one or several genes, especially for rapid radiations, will probably be insufficient. The major sources of the gene tree incongruence we find are low-resolution gene trees and substantial ILS during the rapid radiation. It is possible that some of the deep branches of the species tree are in the anomaly zone (63), although the gene tree support is not high enough to confidently test this idea. It is also possible that some gene and local species tree incongruence could reflect ancient hybridization during the radiation, but distinguishing between this and other sources of hemiplasy (83) would require more complete assemblies, genes without missing data across species, and development of new methods (84). Finally, it is also possible that insufficient taxon sampling contributed to the local species tree incongruence, known to lead to long-branch attraction (70). We did seek to break up some long branches, specifically within core landbirds and core waterbirds. However, the very large-scale data collection for this study made it necessary to prioritize species for specific parts of the tree. Moreover, the potential to add taxa that will break up long branches is limited for a number of groups because the species either are extinct or there are no more major lineages to sample, suggesting that further study of analytical methods for whole genomes will prove to be as important as additional taxa.

Genomic-scale amounts of protein-coding sequence data were not only insufficient but were also misleading for generating an accurate avian phylogeny due to convergence. One possible explanation is convergent GC-biased gene conversion in exons, where AT-GC mismatches are corrected by DNA repair molecules in a biased manner to produce more gametes with the GC allele (85). GC-biased gene conversion correlates with recombination rate (86), and new GC alleles reach fixation more easily in species with larger population sizes, which tend to also have smaller body sizes (87). Recombination also tends to be higher toward the ends of chromosomes (88), where we found higher GC-rich high-variance exons. An alternative possibility is that the associations of ecology and/or life history are related to convergent exon-coding mutations for those traits in avian genomes (89, 90).

With a well-resolved tree, it becomes possible to more confidently infer evolution of convergent traits. Our tree lends support for either three independent gains of vocal learning (38, 91) or two gains (hummingbirds and the common ancestor of parrots and oscine songbirds) followed by two losses (in New Zealand wrens and suboscines) (29, 39). However, a single origin for parrots and oscines followed by two losses (three events) is not much less parsimonious than independent origins in parrots and oscines (two events). In addition, the suboscine *Procnias* bellbirds have recently been shown to be vocal learners (92, 93), suggesting that there could have been a fourth gain or a regain after a loss of vocal learning in other suboscines. The non-monophyly of the birds of prey at the deepest branches of the Australaves and Afroaves radiations suggests that the common ancestor of core landbirds may have been an apex predator, followed by two losses of the raptorial trait. Seriema at the deepest branch of Australaves could be considered to belong to a raptorial taxon because they kill vertebrate prey (94) and are the sole living relatives of the extinct giant "terror birds," apex predators during the Paleogene (95, 96). The deepest branches after Accipitriformes and owl among the Afroaves, the mousebirds and cuckoo-roller, have Eocene relatives with raptor-like feet (97), and the cuckoo-roller specializes on chameleon prey (98). This suggests that losses of the predatory phenotype were gradual across successive divergences of each of the two core landbird radiations. More
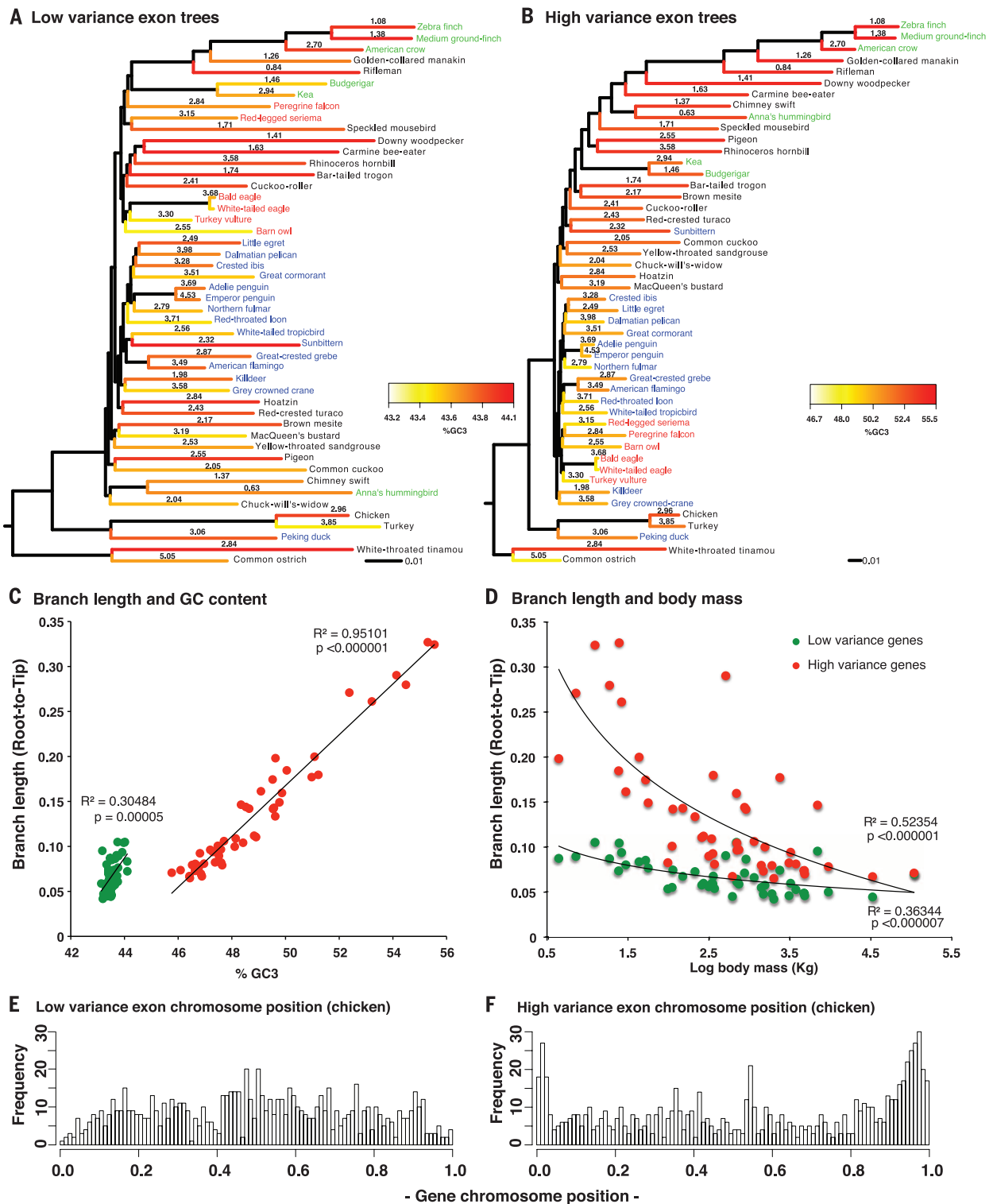
Fig. 6. Life history incongruence in protein-coding trees. (**A**) Species tree inferred from low–base composition variance exons (*n* = 830 genes) graphed with branch length, third codon position GC (GC3) content (heatmap), and log of body mass (numbers on branches). (**B**) Species tree inferred from high–base composition variance exons (*n* = 830 genes), graphed similarly as in (A). The %GC3 scale is higher and ~10 times wider for the high-variance genes, and the branch lengths are ~3 times longer [black scales at the bottom of (A) and (B)]. Color coding of species' names is as in Fig. 1. Cladograms of trees in (A) and (B) are in figs. S16, A and B. (**C** and **D**)

Correlations of branch length with GC content (C) and body mass (D) of the low-variance and high-variance exons. Correlations were still significant after independent contrast analyses for phylogenetic relationships (SM11). (**E** and **F**) Relative chromosome positions of the low-variance (E) and high-variance (F) exons normalized between 0 and 1 for all chicken chromosomes and separated into 100 bins (bars). The height of each bar represents the number of genes in that specific relative location. The two distributions in (E) and (F) are significantly different ($P < 2.2 \times 10^{-16}$, Wilcoxon rank sum test on grouped values). For further details, see SM11.

broadly, the Columbea and Passerea clades appear to have many ecologically driven convergent traits that have led previous studies to group them into supposed monophyletic taxa (*8, 17, 25*). These convergences include the footpropelled diving trait of grebes in Columbea with loons and cormorants (*15*) in Passerea, the wading-feeding trait of flamingos in Columbea with ibises and egrets (*24, 99*) in Passerea, and pigeons and sandgrouse in Columbea with shorebirds (killdeer) in Passerea (*24*). These long-known trait and morphological alliances suggest that some of the traditional nongenomic trait classifications are based on polyphyletic assemblages.

In conclusion, our genome-scale analysis supports the hypothesis of a rapid radiation of diverse species occurring within a relatively short period of time (36 lineages within 10 to 15 million years; Fig. 1) during the K-Pg transition, with many interordinal divergences in the 1- to 3-million-year range. This rate of divergence is consistent with modern speciation rates, but it is notable that so many lineages from a single stem lineage survived extinction. Subsequent ecological diversification of surviving lineages is consistent with a proliferation of the earliest fossil stem representatives of most modern orders by the latest Paleocene to Eocene. Our finding is broadly consistent with recent estimates for placental mammals [(*100*), but see SM12 (*101*)] and thus supports the hypothesis that the K-Pg transition was associated with a rapid species radiation caused by a release of ecological niches following the environmental destruction and species extinctions linked to an asteroid impact (*2, 4, 5, 102*).

REFERENCES AND NOTES

1. C. Venditti, A. Meade, M. Pagel, *Nature* **463**, 349–352 (2010).
2. J. B. Yoder *et al.*, *J. Evol. Biol.* **23**, 1581–1596 (2010).
3. A. Feduccia, *Science* **267**, 637–638 (1995).
4. P. Schulte *et al.*, *Science* **327**, 1214–1218 (2010).
5. N. R. Longrich, T. Tokaryk, D. J. Field, *Proc. Natl. Acad. Sci. U.S.A.* **108**, 15253–15257 (2011).
6. D. T. Ksepka, C. A. Boyd, *Paleobiology* **38**, 112–125 (2012).
7. K. M. Cohen, S. Finney, P. L. Gibbard, International Chronostratigraphic Chart v2013/01, in *International Commission on Stratigraphy* (2013); www.stratigraphy.org/ICSchart/ChronostratChart2013-01.jpg.
8. P. G. Ericson *et al.*, *Biol. Lett.* **2**, 543–547 (2006).
9. R. W. Meredith *et al.*, *Science* **334**, 521–524 (2011).
10. W. Jetz, G. H. Thomas, J. B. Joy, K. Hartmann, A. O. Mooers, *Nature* **491**, 444–448 (2012).
11. O. Haddrath, A. J. Baker, *Proc. Biol. Sci.* **279**, 4617–4625 (2012).
12. M. S. Lee, A. Cau, D. Naish, G. J. Dyke, *Syst. Biol.* **63**, 442–449 (2014).
13. J. W. Brown, J. S. Rest, J. García-Moreno, M. D. Sorenson, D. P. Mindell, *BMC Biol.* **6**, 6 (2008).
14. M. A. Pacheco *et al.*, *Mol. Biol. Evol.* **28**, 1927–1942 (2011).
15. B. C. Livezey, R. L. Zusi, *Zool. J. Linn. Soc.* **149**, 1–95 (2007).
16. G. Mayr, *J. Zool. Syst. Evol. Res.* **49**, 58–76 (2011).
17. S. J. Hackett *et al.*, *Science* **320**, 1763–1768 (2008).
18. R. C. Pratt *et al.*, *Mol. Biol. Evol.* **26**, 313–326 (2009).
19. B. Nabholz, A. Künstner, R. Wang, E. D. Jarvis, H. Ellegren, *Mol. Biol. Evol.* **28**, 2197–2210 (2011).
20. O. Jeffroy, H. Brinkmann, F. Delsuc, H. Philippe, *Trends Genet.* **22**, 225–231 (2006).
21. S. Song, L. Liu, S. V. Edwards, S. Wu, *Proc. Natl. Acad. Sci. U.S.A.* **109**, 14942–14947 (2012).
22. J. Alföldi, K. Lindblad-Toh, *Genome Res.* **23**, 1063–1068 (2013).
23. J. L. Peters, *Check-List of Birds of the World*, E. Mayr, R. A. Paynter, M. A. Traylor, J. C. Greenway, Eds. (Harvard Univ. Press, Cambridge, MA, 1937–1987).
24. C. G. Sibley, J. E. Ahlquist, *Phylogeny and Classification of Birds: A Study in Molecular Evolution* (Yale Univ. Press, New Haven, CT, 1990).
25. M. G. Fain, P. Houde, *Evolution* **58**, 2558–2573 (2004).
26. N. Wang, E. L. Braun, R. T. Kimball, *Mol. Biol. Evol.* **29**, 737–750 (2012).
27. R. T. Kimball, N. Wang, V. Heimer-McGinn, C. Ferguson, E. L. Braun, *Mol. Phylogenet. Evol.* **69**, 1021–1032 (2013).
28. J. E. McCormack *et al.*, *PLOS ONE* **8**, e54848 (2013).
29. A. Suh *et al.*, *Nat. Commun.* **2**, 443 (2011).
30. M. T. Mahmood, P. A. McLenachan, G. C. Gibb, D. Penny, *Genome Biol. Evol.* **6**, 326–332 (2014).
31. A. Matzke *et al.*, *Mol. Biol. Evol.* **29**, 1497–1501 (2012).
32. J. L. Chojnowski, R. T. Kimball, E. L. Braun, *Gene* **410**, 89–96 (2008).
33. S. Patel, R. T. Kimball, E. L. Braun, *J. Phylogenetics Evol. Biol.* **1**, 9–10 (2013).
34. Y. I. Wolf, I. B. Rogozin, N. V. Grishin, E. V. Koonin, *Trends Genet.* **18**, 472–479 (2002).
35. A. Rokas, B. L. Williams, N. King, S. B. Carroll, *Nature* **425**, 798–804 (2003).
36. J. Cracraft, in *The Howard and Moore Complete Checklist of the Birds of the World*, E. C. Dickinson, J. V. Remsen, Eds. (Aves Press, Eastbourne, UK, 2013), pp. xxi–xliii.
37. E. C. Dickinson, J. V. Remsen, Eds., *The Howard and Moore Complete Checklist of Birds of the World* (Aves Press, Eastbourne, UK, 2013).
38. E. D. Jarvis, *Ann. N.Y. Acad. Sci.* **1016**, 749–777 (2004).
39. D. F. Clayton, C. N. Balakrishnan, S. E. London, *Curr. Biol.* **19**, R865–R873 (2009).
40. L. W. Hillier *et al.*, *Nature* **432**, 695–716 (2004).
41. R. A. Dalloul *et al.*, *PLOS Biol.* **8**, e1000475 (2010).
42. W. C. Warren *et al.*, *Nature* **464**, 757–762 (2010).
43. J. Alföldi *et al.*, *Nature* **477**, 587–591 (2011).
44. G. Zhang *et al.*, *Science* **346**, 1311–1320 (2014).
45. M. D. Shapiro *et al.*, *Science* **339**, 1063–1067 (2013).
46. X. Zhan *et al.*, *Nat. Genet.* **45**, 563–566 (2013).
47. Y. Huang *et al.*, *Nat. Genet.* **45**, 776–783 (2013).
48. Z. Wang *et al.*, *Nat. Genet.* **45**, 701–706 (2013).
49. G. Ganapathy *et al.*, *Gigascience* **3**, 11 (2014).
50. S. Li *et al.*, *Genome Biol.* 10.1186/s13059-014-0557-1 (2014).
51. C. Li *et al.*, *GigaScience* **3**, 27 (2014).
52. R. E. Green *et al.*, *Science* **346**, 1254449 (2014).
53. K. Liu, S. Raghavan, S. Nelesen, C. R. Linder, T. Warnow, *Science* **324**, 1561–1564 (2009).
54. K. Liu *et al.*, *Syst. Biol.* **61**, 90–106 (2012).
55. A. Stamatakis *et al.*, *Bioinformatics* **28**, 2064–2066 (2012).
56. J. Zhang, A. Stamatakis, "The multi-processor scheduling problem in phylogenetics," *IEEE 26th International Parallel and Distributed Processing Symposium*, Shanghai, 21 to 25 May 2012, pp. 691–698; 10.1109/IPDPSW.2012.86.
57. A. Stamatakis, A. J. Aberer, "Novel parallelization schemes for large-scale likelihood-based phylogenetic inference," *IEEE 27th International Symposium on Parallel and Distributed Processing*, Boston, 20 to 24 May 2013, pp. 1195–1204; 10.1109/IPDPS.2013.70.
58. S. Mirarab, M. S. Bayzid, B. Boussau, T. Warnow, *Science* **346**, 1250463 (2014).
59. T. Yuri *et al.*, *Biology (Basel)* **2**, 419–444 (2013).
60. P. G. Ericson, *J. Biogeogr.* **39**, 813–824 (2012).
61. J. Kim, *Mol. Phylogenet. Evol.* **17**, 58–75 (2000).
62. W. P. Maddison, *Syst. Biol.* **46**, 523–536 (1997).
63. N. A. Rosenberg, *Mol. Biol. Evol.* **30**, 2709–2713 (2013).
64. J. H. Degnan, N. A. Rosenberg, *Trends Ecol. Evol.* **24**, 332–340 (2009).
65. A. W. Edwards, *Genetics* **183**, 5–12 (2009).
66. M. S. Bayzid, T. Warnow, *Bioinformatics* **29**, 2277–2284 (2013).
67. L. Liu, L. Yu, S. V. Edwards, *BMC Evol. Biol.* **10**, 302 (2010).
68. J. Huerta-Cepas, S. Capella-Gutiérrez, L. P. Pryszcz, M. Marcet-Houben, T. Gabaldón, *Nucleic Acids Res.* **42**, D897–D902 (2014).
69. M. P. Simmons, H. Ochoterena, *Syst. Biol.* **49**, 369–381 (2000).
70. J. Felsenstein, *Inferring Phylogenies* (Sinauer Associates, Sunderland, MA, 2004).
71. J. C. Avise, T. J. Robinson, *Syst. Biol.* **57**, 503–507 (2008).
72. D. A. Ray, J. Xing, A. H. Salem, M. A. Batzer, *Syst. Biol.* **55**, 928–935 (2006).
73. K. L. Han *et al.*, *Syst. Biol.* **60**, 375–386 (2011).
74. E. M. Lemmon, A. R. Lemmon, *Annu. Rev. Ecol. Evol.* **44**, 99–121 (2013).
75. C. C. Weber, B. Boussau, J. Romiguier, E. D. Jarvis, H. Ellegren, *Genome Biol.* **15**, 549 (2014).
76. C. C. Weber, B. Nabholz, J. Romiguier, H. Ellegren, *Genome Biol.* **15**, 542 (2014).
77. M. dos Reis, Z. Yang, *Mol. Biol. Evol.* **28**, 2161–2172 (2011).
78. J. V. Smith, E. L. Braun, R. T. Kimball, *Syst. Biol.* **62**, 35–49 (2013).
79. P. Houde, *Nature* **324**, 563–565 (1986).
80. G. Mayr, *Syst. Biodivers.* **11**, 7–13 (2014).
81. J. A. Clarke, C. P. Tambussi, J. I. Noriega, G. M. Erickson, R. A. Ketcham, *Nature* **433**, 305–308 (2005).
82. L. Salichos, A. Rokas, *Nature* **497**, 327–331 (2013).
83. L. Salichos, A. Stamatakis, A. Rokas, *Mol. Biol. Evol.* **31**, 1261–1271 (2014).
84. A. D. Twyford, R. A. Ennos, *Heredity (Edinb.)* **108**, 179–189 (2012).
85. L. Duret, N. Galtier, *Annu. Rev. Genomics Hum. Genet.* **10**, 285–311 (2009).
86. C. F. Mugal, P. F. Arndt, H. Ellegren, *Mol. Biol. Evol.* **30**, 1700–1712 (2013).
87. J. Romiguier, V. Ranwez, E. J. Douzery, N. Galtier, *Genome Res.* **20**, 1001–1009 (2010).
88. M. K. Rudd *et al.*, *PLOS Genet.* **3**, e32 (2007).
89. J. Parker *et al.*, *Nature* **502**, 228–231 (2013).
90. Proteome-wide analyses among the 48 bird genomes were conducted in (*44*), where it was found that vocal-learning bird species have convergent amino acid changes in a set of genes expressed in the song-learning nuclei.
91. F. Nottebohm, *Am. Nat.* **106**, 116–140 (1972).
92. V. Saranathan, D. Hamilton, G. V. Powell, D. E. Kroodsma, R. O. Prum, *Mol. Ecol.* **16**, 3689–3702 (2007).
93. D. Kroodsma *et al.*, *Wilson J. Ornithol.* **125**, 1–14 (2013).
94. K. H. Redford, G. Peters, *J. Field Ornithol.* **57**, 261–269 (1986).
95. H. M. F. Alvarenga, E. Hofling, *Papeis Avulsos Zool.* **43**, 55–91 (2003).
96. G. Mayr, in *Paleogene Fossil Birds* (Springer, Berlin, Heidelberg, 2009), pp. 139–152.
97. P. Houde, S. L. Olson, in *Natural History Museum of Los Angeles County Science Series* (Natural History Museum of Los Angeles County, Los Angeles, 1992), vol. 36, pp. 137–160.
98. A. D. Forbes-Watson, *Ibis* **109**, 425–430 (1967).
99. S. L. Olson, A. Feduccia, *Smithson. Contrib. Zool.* **316**, 1–73 (1980).
100. M. A. O'Leary *et al.*, *Science* **339**, 662–667 (2013).
101. M. dos Reis, P. C. Donoghue, Z. Yang, *Biol. Lett.* **10**, 20131003 (2014).
102. M. J. Benton, *Philos. Trans. R. Soc. Lond. B Biol. Sci.* **365**, 3667–3679 (2010).

TECHNICAL COMMENT

AVIAN GENOMICS

Comment on "Whole-genome analyses resolve early branches in the tree of life of modern birds"

Kieren J. Mitchell,[1]* Alan Cooper,[1] Matthew J. Phillips[2]

Jarvis *et al.* (Research Articles, 12 December 2014, p. 1320) presented molecular clock analyses that suggested that most modern bird orders diverged just after the mass extinction event at the Cretaceous-Paleogene boundary (about 66 million years ago). We demonstrate that this conclusion results from the use of a single inappropriate maximum bound, which effectively precludes the Cretaceous diversification overwhelmingly supported by previous molecular studies.

Substantial discrepancies exist between the first appearance in the fossil record of many avian lineages and their age as estimated by molecular clock analyses (1). A particularly contentious topic is the time scale for the divergences between modern bird orders (2). The oldest fossil generally agreed to fall within Neornithes—the clade comprising all living birds (Fig. 1A)—is *Vegavis* (3), from the end-Cretaceous ~67 million years ago (Ma). However, most molecular dating studies have suggested that Neornithes began diversifying more than 110 Ma (4–6). Conversely, Jarvis *et al.* (7) presented genome-based molecular clock results that supported predominantly post-Cretaceous dates for the diversification of modern birds.

Although Jarvis *et al.*'s genomic data set and phylogeny are impressive leaps forward for the field, the influence of their calibrations requires closer investigation. Their phylogeny was calibrated by applying minimum and maximum bounds to key nodes. Best-practice approaches for defining minimum bounds are well established (8, 9): The origin of a clade necessarily predates the appearance of its first unequivocal fossil representative. However, maximum bounds (the earliest plausible age of a clade) are a more difficult proposition, yet just as important for estimating dates (10, 11).

Jarvis *et al.*'s only maximum age constraint among birds (the root of Neornithes) was weakly justified. They implemented a strong prior against the diversification of Neornithes occurring before the Late Cretaceous (99.6 Ma). This decision effectively precluded results consistent with many previous molecular clock studies, which have generally recovered ages for Neornithes between 110 and 140 Ma (4–6). Their first justification for the 99.6-Ma bound, that it is 30 million years

older than their age estimate for Neoaves (two nodes shallower), is immaterial. Their second justification, that the bound "far exceeds the age of paleontological evidence for the existence of Neornithes" [supplementary materials for (7)] [e.g., the putative neornithine, *Austinornis* at ~85 Ma (12)], is only relevant if it covers relatively well-sampled fossil assemblages in potential geographic areas of origin that contain no putative clade members but do preserve ancestral forms or ecological equivalents (10, 13). However, the few fossils attributable to Euornithes (neornithines and their close relatives) (see Fig. 1A) during this period (from ~85 Ma to Jarvis *et al.*'s maximum at 99.6 Ma) are taphonomically biased, including only a handful of seabirds (14). Because early neornithines may well have been terrestrial (Fig. 1A), assigning a maximum constraint based on this Late Cretaceous record is clearly inappropriate.

We reanalyzed Jarvis *et al.*'s molecular dating data set (722,202 nucleotides from 51 diapsid species, including 48 birds) using the authors' total evidence nucleotide tree (TENT) topology, while varying the maximum bound for Neornithes. Our analyses were otherwise performed according to the methods described in the original study.

Recent studies have used the absence of neornithines from some Early Cretaceous deposits, where the avian fossil record is far superior, to set a 97.5% prior maximum bound of 117.5 Ma (5). When we reanalyzed Jarvis *et al.*'s genomic data with this more appropriate maximum bound, the number of sampled neornithines with pre–Cretaceous-Paleogene (K-Pg) mean divergence estimates increased from 15 to 22 out of 47 [nodes with 95% highest posterior densities (HPDs) entirely pre–K-Pg increased from 10 to 13], and the posterior mean for the origin of modern birds fell close to the maximum, at 117.2 Ma (Fig. 1B).

However, even this older maximum constraint remains inappropriate if modern birds were ini-

tially restricted to Gondwana, as is presently the case for most basal neornithine clades, including ratites, megapodes, cracids, and screamers. Within Late Cretaceous Gondwana, the oldest bird fossil is a putative neornithine (15), and the known Early Cretaceous Gondwanan fossil record is largely uninformative, containing only the non-euornithine *Nanantius* and taxonomically indeterminate fragments. When such potential geographic origins are considered, it becomes difficult to justify even a 117.5-Ma maximum. Removing the maximum bound on Neornithes altogether resulted in pre–K-Pg mean estimates for a full 37 of our 47 neornithine divergences (29 nodes with 95% HPDs entirely pre–K-Pg), and the posterior mean for the origin of modern birds increased to 162.5 Ma (Fig. 1B). This date is substantially older even than *Archaeopteryx*, suggesting that substitution or rate variation models are misspecified.

In summary, Jarvis *et al.* (7) employed a strong maximum constraint on the age of Neornithes that is poorly supported by the fossil record and that heavily influenced their inference of post-Cretaceous bird diversification. Without imposing this constraint, their genomic data and remaining calibrations favor deep Neornithes origins, with most interordinal divergences occurring in the Cretaceous, consistent with previous molecular dating studies. If indeed the major diversification of modern birds occurred after the K-Pg mass extinction event, which arguably better fits the fossil record, it could be explained by parallel rate decelerations across modern avian clades being nonidentifiable even to relaxed clock methods. However, support for such agreement with fossil records must come from improvements in either the model of molecular rate variation or better fossil sampling and not from the imposition of artificially strong maximum age constraints.

REFERENCES AND NOTES

1. D. T. Ksepka, J. L. Ware, K. S. Lamm, *Proc. Biol. Sci.* **281**, 20140677 (2014).
2. G. Mayr, *Palaeontology* **57**, 231–242 (2014).
3. J. A. Clarke, C. P. Tambussi, J. I. Noriega, G. M. Erickson, R. A. Ketcham, *Nature* **433**, 305–308 (2005).
4. O. Haddrath, A. J. Baker, *Proc. Biol. Sci.* **279**, 4617–4625 (2012).
5. W. Jetz, G. H. Thomas, J. B. Joy, K. Hartmann, A. O. Mooers, *Nature* **491**, 444–448 (2012).
6. J. W. Brown, J. S. Rest, J. García-Moreno, M. D. Sorenson, D. P. Mindell, *BMC Biol.* **6**, 6 (2008).
7. E. D. Jarvis *et al.*, *Science* **346**, 1320–1331 (2014).
8. R. R. Reisz, J. Müller, *Trends Genet.* **20**, 237–241 (2004).
9. J. F. Parham *et al.*, *Syst. Biol.* **61**, 346–359 (2012).
10. M. J. Phillips, *Palaeontol. Electronica* **2015**, 18.1.5FC (2015).
11. L. A. Hug, A. J. Roger, *Mol. Biol. Evol.* **24**, 1889–1897 (2007).
12. T. S. Myers, *J. Paleontol.* **84**, 1071–1081 (2010).
13. R. Barnett *et al.*, *Curr. Biol.* **15**, R589–R590 (2005).
14. The data were downloaded from the Paleobiology Database (https://paleobiodb.org) on 5 March 2015.
15. F. L. Agnolin, F. E. Novas, G. Lio, *Ameghiniana* **43**, 245–248 (2006).

[1]Australian Centre for Ancient DNA, School of Biological Sciences, University of Adelaide, Australia. [2]School of Earth, Environmental, and Biological Sciences, Queensland University of Technology, Brisbane, Australia.
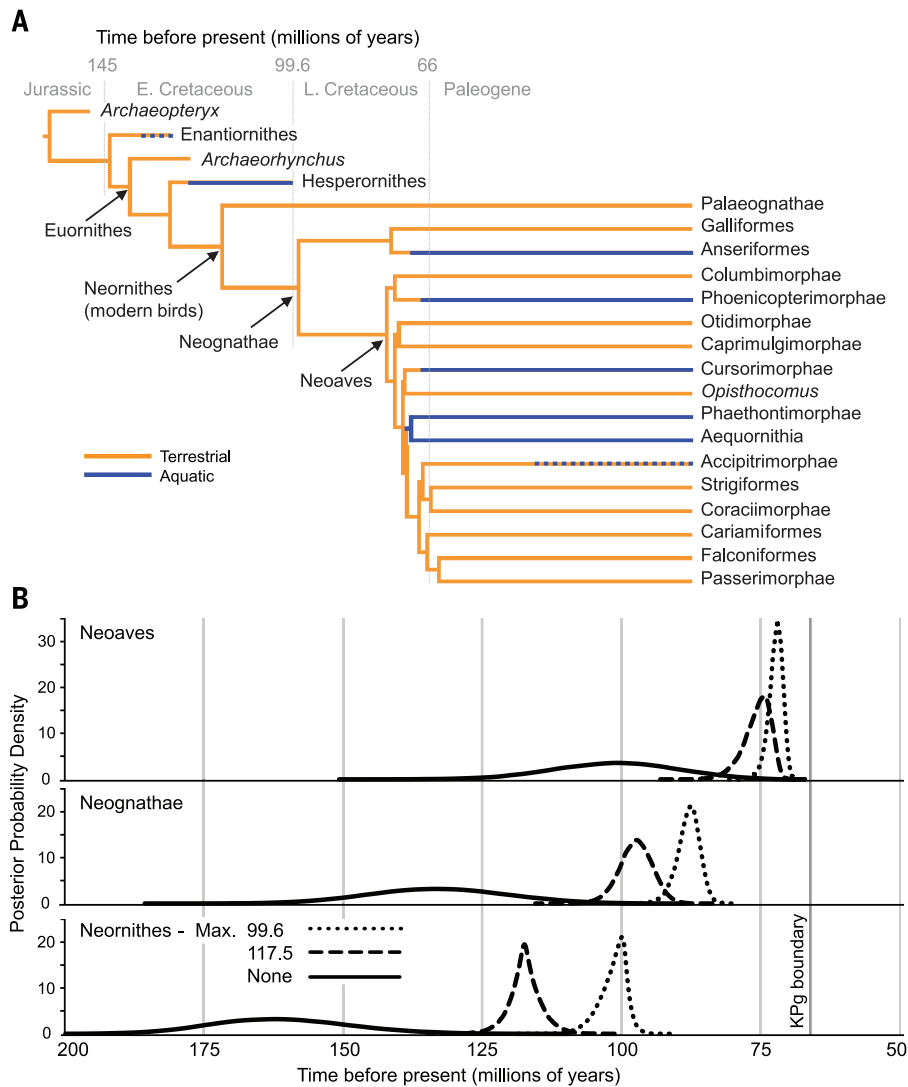*Corresponding author. E-mail: kieren.mitchell@adelaide.edu.au

Fig. 1. Reanalysis of Jarvis *et al.*'s genomic data set. (**A**) Jarvis *et al.*'s TENT topology (partially collapsed for clarity) placed into temporal context with the earliest records for several older avian lineages. Divergence dates among living species are derived from analyses following Jarvis *et al.* (*7*) but employ a more appropriate 117.5-Ma maximum bound for the diversification of neornithines. In addition, ancestral habitat was reconstructed under maximum parsimony for terrestrial (orange) and aquatic (blue) lineages, with approximate transition times based on fossil records. Dotted lines indicate the existence of derived aquatic taxa within a clade for which terrestriality appears ancestral. (**B**) Posterior age distributions for several key nodes under three different maxima for Neornithes: 99.6 Ma (dotted line), 117.5 Ma (dashed line), and removal of this maximum constraint (solid line).

TECHNICAL RESPONSE

AVIAN GENOMICS

Response to Comment on "Whole-genome analyses resolve early branches in the tree of life of modern birds"

Joel Cracraft,[1]*† Peter Houde,[2]* Simon Y. W. Ho,[3]* David P. Mindell,[4] Jon Fjeldså,[5]
Bent Lindow,[6] Scott V. Edwards,[7] Carsten Rahbek,[8,9] Siavash Mirarab,[10]
Tandy Warnow,[10,11] M. Thomas P. Gilbert,[6,12] Guojie Zhang,[13,14]
Edward L. Braun,[15]† Erich D. Jarvis[16,17]†

Mitchell *et al.* argue that divergence-time estimates for our avian phylogeny were too young because of an "inappropriate" maximum age constraint for the most recent common ancestor of modern birds and that, as a result, most modern bird orders diverged before the Cretaceous-Paleogene mass extinction event 66 million years ago instead of after. However, their interpretations of the fossil record and timetrees are incorrect.

It is well known that changing the prior maximum age constraint in a Bayesian relaxed clock analysis can change estimates of species divergence times (*1*). Jarvis *et al.* (*2*) estimated the rapid diversification of Neoaves to be near the Cretaceous-Paleogene (K-Pg) boundary based on data-rich analyses, including first and second codon positions of 1156 clocklike nuclear genes, 19 internal fossil calibrations, and a maximum age constraint of 99.6 million years ago (Ma) on the most recent common ancestor (MRCA) of Neornithes (modern birds) based on the Early-Late Cretaceous boundary. Mitchell *et al.* (*3*) claim that our 99.6-Ma constraint was "inappropriate." Their contention is, instead, that a maximum constraint at 117.5 Ma—well into the Early Cretaceous (~145 to 99.6 Ma)—is "more appropriate," and upon applying it, they unsurprisingly found that many divergences moved deeper in time, thus implying a major radiation of Neoaves in the Late Cretaceous (~99.6 to 66 Ma) before the 66-Ma K-Pg mass extinction event. Evaluating Mitchell *et al.*'s arguments requires answers to two questions: (i) is the maximum age constraint they used more appropriate than that used by Jarvis *et al.* (*2*) and (ii) does the use of different constraints for the MRCA of Neornithes substantially alter conclusions regarding timing of the neoavian radiation?

Addressing question (i), although Mitchell *et al.* claim that their 117.5-Ma prior is more appropriate, in fact it is a calibration product of the Early Cretaceous (110 Ma) fossil *Gansus yumenensis* (*4*) and a prior probability density chosen by Jetz *et al.* (*5*), rather than direct fossil evidence. Further, *Gansus* is an ornithurine (*4*) lying far outside other Mesozoic fossils more closely related to Neornithes (*6*, *7*) and thus is an inappropriately old constraint for dating modern birds. Consequently, the empirical basis for their calibration is not well justified.

Mitchell *et al.* criticize our use of the empirical fossil record on the grounds that the record is taphonomically biased across space and time due to poor preservation of Southern Hemisphere Late Cretaceous terrestrial avian fossils, which they infer represent the most basal neornithines. Although

the Northern Hemisphere is better sampled than the Southern Hemisphere (*8*), small terrestrial non-neornithine birds ecologically equivalent to terrestrial neornithines are conspicuous in the Late Cretaceous avifaunas from Argentina (*9*) and Madagascar (*10*), whereas neornithines are conspicuously absent. Moreover, based on their survey of the avian fossil record, Fountaine *et al.* (*11*) conclude that "it is unlikely that the modern clades would have remained independently cryptic throughout [the Late Cretaceous]."

Mitchell *et al.* also largely dismiss the Early Cretaceous fossil record as uninformative with respect to the origin of neornithines, but then call attention to several fossils from the beginning of the Late Cretaceous to bolster their argument for an Early Cretaceous origin. We believe, however, that their interpretations of these fossils are faulty. Mitchell *et al.* refer to *Austinornis* at 85 Ma and cite Myers (*12*). However, Myers (*12*) does not mention *Austinornis* or an 85-Ma age for it. Clarke (*13*), on the other hand, while noting that *Austinornis lentus* has one character that suggests it might be a stem-galliform, stresses that this fossil should not be used in dating analyses (it lacked 99% of the characters in her matrix). Mitchell *et al.* raise the issue of a putative neornithine fossil from Patagonia ~83 to 94 Ma (*14*). However, the neornithine relationships of this fragmentary fossil are uncertain (*15*), and even if it were a neornithine, there would be no inconsistency with our results. Our results are consistent with the most convincing pre–K-Pg Neornithes fossil to date, *Vegavis*, a very Late Cretaceous (66 to 68 Ma) (*16*) inferred stem-anseriform (*2*). In contrast, the diverse and well-preserved Jehol Biota of China, which provides a window into a ~130 to 120 Ma Early Cretaceous period (*17*), has never yielded a neornithine fossil. The issue is not whether fossils assignable to the avian crown group (Neornithes) will be found in the Early to Late Cretaceous but that, with the exception of *Vegavis,* they have not been documented. The fossil record does not support the presence of a diverse Neornithine avifauna in the Early or Late Cretaceous, and especially not of Neoaves, the focus of Jarvis *et al.* (*2*).

To address question (ii), we examined the sensitivity of our relaxed clock analyses to different maximum age constraints for Neornithes in more detail. We note that even younger age constraints have been proposed (*18*), which Jarvis *et al.* (*2*) examined. Comparing results from all three proposed maximum constraints of 86.5 (*18*), 99.6 (*2*), and 117.5 Ma (*3*), among the 37 divergences of major ordinal lineages in Neoaves, only 1 to 4 out of 37 (3 to 11%), 5 to 9 out of 37 (14 to 24%) and 10 to 15 out of 37 (31 to 41%), respectively, predate the K-Pg boundary (Fig. 1, A to C) (mean dates). The exact numbers of divergences pre–K-Pg vary slightly depending on parameters and stochasticity of software dating methods (see figure legend) and the exact date used for the K-Pg, since so many divergences are near it. Importantly, the 95% credibility intervals (CI) showed that few divergences were exclusively pre–K-Pg boundary (0, 8, and 14%) under all three constraints, whereas the vast majority of CIs overlapped with the

[1]Department of Ornithology, American Museum of Natural History, New York, NY 10024, USA. [2]Department of Biology, New Mexico State University, Las Cruces, NM 88003, USA. [3]School of Biological Sciences, University of Sydney, Sydney, New South Wales 2006, Australia. [4]Department of Biochemistry and Biophysics, University of California, San Francisco, CA 94158, USA. [5]Center for Macroecology, Evolution and Climate, Natural History Museum of Denmark, University of Copenhagen, Universitetsparken 15, DK-2100 Copenhagen Ø, Denmark. [6]Centre for GeoGenetics, Natural History Museum of Denmark, University of Copenhagen, Øster Voldgade 5-7, 1350 Copenhagen, Denmark. [7]Department of Organismic and Evolutionary Biology and Museum of Comparative Zoology, Harvard University, Cambridge, MA 02138, USA. [8]Center for Macroecology, Evolution and Climate, Natural History Museum of Denmark, University of Copenhagen, Universitetsparken 15, DK-2100 Copenhagen Ø, Denmark. [9]Department of Life Sciences, Imperial College London, Silwood Park Campus, Ascot SL5 7PY, UK. [10]Department of Computer Science, The University of Texas at Austin, Austin, TX 78712, USA. [11]Departments of Bioengineering and Computer Science, University of Illinois at Urbana-Champaign, Urbana, IL 61801, USA. [12]Trace and Environmental DNA Laboratory Department of Environment and Agriculture, Curtin University, Perth, Western Australia 6102, Australia. [13]China National GeneBank, BGI-Shenzhen, Shenzhen 518083, China. [14]Centre for Social Evolution, Department of Biology, Universitetsparken 15, University of Copenhagen, DK-2100 Copenhagen, Denmark. [15]Department of Biology and Genetics Institute, University of Florida, Gainesville, FL 32611, USA. [16]Department of Neurobiology, Duke University Medical Center, Durham, NC 27710, USA. [17]Howard Hughes Medical Institute, Chevy Chase, MD 20815, USA.
*These authors contributed equally to this work. †Corresponding author. E-mail: jlc@amnh.org (J.C.); ebraun68@ufl.edu (E.L.B.); jarvis@neuro.duke.edu (E.D.J.)
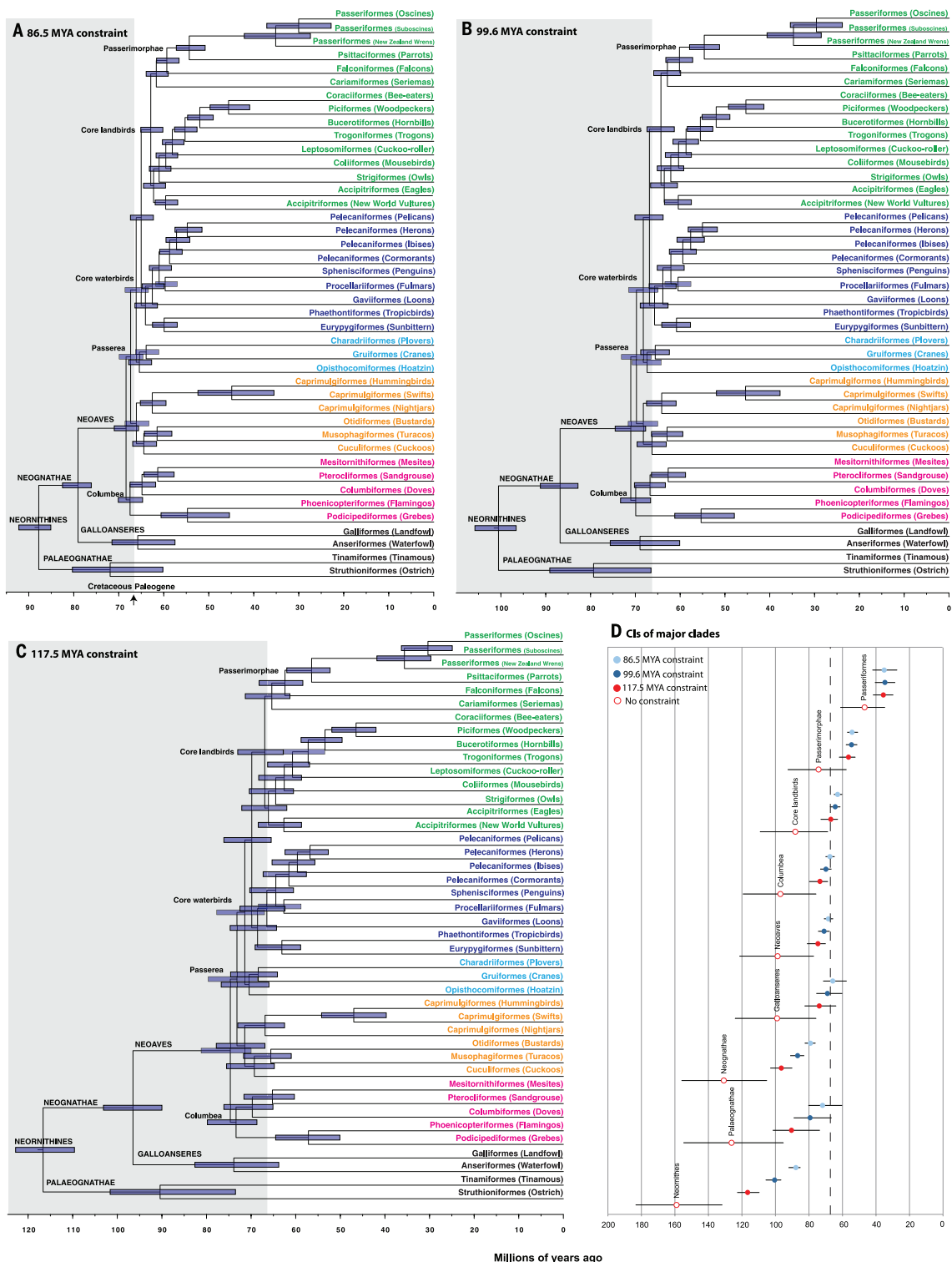
Fig. 1 Genome-scale avian timetrees with 95% CIs and different maximum age constraints for Neornithes. (**A** to **C**) Timetrees using the 86.5, 99.6, and 117.5 Ma maximum constraints, respectively, on exons of 1156 clocklike genes and the most recent version of the MCMCTREE program (*20*). The 95% CIs (blue bars) in (A) and (B) are slightly narrower and some divergences moved backward or forward in time by approximately one million years compared with those in Jarvis *et al.* (*2*), as a result of stochastic MCMC sampling effects and using an updated version of the software. However, the overall results are similar and all lie within the previously defined 95% CIs. Branches with multiple species in the same suborder have been collapsed, and the reptilian outgroups (lizard, turtle, and alligator) are not shown. We do not show the four extinct lineages included in the Mitchell *et al.* (*3*) tree because they are not directly used in the Bayesian dating analysis. Order/suborder names are color coded according to large monophyletic groups. (**D**) Comparison of dates and 95% CIs for key avian divergences using the different maximum constraints. There are no dramatic shifts in dates beyond the Neornithes, Palaeognathae, and Neognathae splits, unless one eliminates the maximum age constraint for Neornithes altogether. MYA, million years ago.

K-Pg (24, 32, and 57%) or were exclusively post–K-Pg (76, 60, and 30%) (Fig. 1, A to D). Thus, most divergences are very near the K-Pg boundary, not many millions of years before. Removing the maximum age constraint altogether results in much earlier divergence-time estimates (Fig. 1D). However, such removal is difficult to justify given the absence of Early Cretaceous neornithine fossils. Inappropriately, Mitchell *et al.* try to contradict our conclusions using divergence dates for all Neornithes in the tree, when our claim was only about Neoaves (*2*). Moreover, they collapsed the branches of nearly all post–K-Pg ordinal divergences into deeper ones, making it appear that most divergences were pre–K-Pg.

In summary, our previous conclusion that Neoaves underwent a rapid radiation near the K-Pg boundary is well founded. Although the estimated dates of the origins of Neornithes and Neognathae do vary with the choice of maximum age constraints, the divergence times for Neoaves are much less sensitive. Improvements to relaxed clock methods may further reduce error due to model fit, but the interpretation of the fossil record will remain the most important component of relaxed clock analyses (*19*). The extremely short branch lengths at the base of Neoaves, along with the evidence for discordance among gene trees due to incomplete lineage sorting [figure 3 in Jarvis *et al.* (*2*)], support what many previous analyses have found, that Neoaves underwent a very rapid radiation near the K-Pg boundary. Such rapid radiations are often associated with ecological drivers. The K-Pg Chicxulub asteroid impact with global ecological changes and mass extinctions around 66 Ma is consistent with its being one potential driver.

REFERENCES AND NOTES

1. R. C. M. Warnock, Z. Yang, P. C. J. Donoghue, *Biol. Lett.* **8**, 156–159 (2012).
2. E. D. Jarvis *et al.*, *Science* **346**, 1320–1331 (2014).
3. K. J. Mitchell, A. Cooper, M. J. Phillips, *Science* **349**, 1460 (2015).
4. H. L. You *et al.*, *Science* **312**, 1640–1643 (2006).
5. W. Jetz, G. H. Thomas, J. B. Joy, K. Hartmann, A. O. Mooers, *Nature* **491**, 444–448 (2012).
6. J. K. O'Connor, Z. Zhou, *J. Syst. Palaeontology* **11**, 889–906 (2013).
7. M. S. Y. Lee, A. Cau, D. Naish, G. J. Dyke, *Syst. Biol.* **63**, 442–449 (2014).
8. L. M. Chiappe, L. M. Witmer, *Mesozoic Birds: Above the Heads of Dinosaurs* (University of California Press, Berkeley, 2002).
9. C. A. Walker, G. J. Dyke, *Isr. J. Earth Sci.* **27**, 15–62 (2009).
10. P. M. O'Connor, C. A. Forster, *J. Vertebr. Paleontol.* **30**, 1178–1201 (2010).
11. T. M. R. Fountaine, M. J. Benton, G. J. Dyke, R. L. Nudds, *Proc. Biol. Sci.* **272**, 289–294 (2005).
12. T. S. Myers, *J. Paleontol.* **84**, 1071–1081 (2010).
13. J. A. Clarke, *Bull. Am. Mus. Nat. Hist.* **286**, 1–179 (2004).
14. F. L. Agnolin, F. E. Novas, *Paläont. Zeit* **86**, 85–89 (2012).
15. G. Mayr, *Paleogene Fossil Birds* (Springer, Berlin, Heidelberg, 2009).
16. J. A. Clarke, C. P. Tambussi, J. I. Noriega, G. M. Erickson, R. A. Ketcham, *Nature* **433**, 305–308 (2005).
17. M. Wang *et al.*, *Nat. Commun.* **6**, 6987 (2015).
18. M. J. Benton, P. C. J. Donoghue, R. J. Asher, in *The Timetree of Life*, S. B. Hedges, S. Kumar, Eds. (Oxford Univ. Press, New York, 2009), pp. 35–86.
19. S. Y. W. Ho, *Trends Ecol. Evol.* **29**, 496–503 (2014).
20. M. Dos Reis, T. Zhu, Z. Yang, *Syst. Biol.* **63**, 555–565 (2014).